Chapter 7
Carbon Dioxide as C-1 Block for the Synthesis of Polycarbonates

Peter T. Altenbuchner, Stefan Kissling, and Bernhard Rieger

Abbreviations

BDI	β-diiminate
BO	1-butene-oxide
CHC	cyclohexene carbonate
CHO	cyclohexene oxide
DFT	density functional theory
DMAP	Dimethylaminopyridine
DNP	2,4-dinitrophenolate
OAc	acetate
PC	propylene carbonate
PDI	Polydispersity index
PCHC	poly(cyclohexene carbonate)
PO	propylene oxide
PPC	poly(propylene carbonate)
PPNCl	*bis*(triphenylphosphine)iminium chloride
TBD	1,5,7-triabicyclo[4,4,0]dec-5-ene
T_g	glass transition temperature
T_m	melting point
TMS	Trimethylsilyl-
TOF	turn-over frequency
TON	turn-over number
VCHC	vinylcyclohexene oxide

P.T. Altenbuchner • S. Kissling • B. Rieger (✉)
Technische Universität München, WACKER-Lehrstuhl für Makromolekulare Chemie, Lichtenbergstrasse 4, Garching 85748, Germany
e-mail: rieger@tum.de

B.M. Bhanage and M. Arai (eds.), *Transformation and Utilization of Carbon Dioxide*, Green Chemistry and Sustainable Technology, DOI 10.1007/978-3-642-44988-8_7,

ZnAA zinc-adipate
ZnGA zinc-glutarate
ZnPA zinc-pimelate
ZnSA zinc-succinate

7.1 Introduction

Fossil energy sources became the dominant energy carriers at the beginning of the twentieth century. Since then, no alternatives to crude oil, gas, and coal have arisen to supplant them as a universal source of energy and raw materials for the chemical industry [1, 2]. The discovery of versatile possibilities for the use of crude oil as well as its low price and historical abundance made the steep rise in living standards in the last 100 years possible. As a result, the concentration of carbon dioxide in the atmosphere has risen significantly and reached 397 ppm in 2013 [3]. However, the finiteness of coal, gas, and especially oil reserves and the steadily increasing demand for them are likely to create a rising imbalance of supply and demand. Furthermore, the various negative implications of reliance on fossil energy carriers generate only limited incentives for industry and consumers to change their accustomed behavior. The reason for the disproportionate low price of CO_2 is that the resulting environmental damage is not or is only partially included in it. The rising generation of carbon dioxide however opens up a vast C-1 source for the synthesis of chemical raw materials. The attractive properties of CO_2 as a nontoxic, renewable, and low-cost C_1-building block are known, and it is currently used on an industrial scale in the production of urea (146×10^6 t/a), methanol (6×10^6 t/a), cyclic carbonate (0.040×10^6 t/a), and salicylic acid (0.060×10^6 t/a), among others [4]. However, the thermodynamic stability has thus far hampered its usage as widespread chemical reagent. Methods to overcome the high energy barriers are based upon reduction, oxidative coupling with unsaturated compounds on low valency metal complexes, and increasing electrophilicity of the carbonyl carbon [5].

The reaction of CO_2 with highly reactive substrates, such as epoxides, affords materials which can be produced on industrially relevant scale (Fig. 7.1). These polycarbonates from CO_2 have the potential to be the next industrial product with a high impact on the usage as commodity polymers. Consequently, the synthesis of highly active catalysts and understanding their mechanistic behavior is of upmost importance and the current developments will be discussed in this chapter.

7.2 Current Situation

Over 20 chemical reaction pathways for carbon dioxide have been developed over the course of the last two decades. Industrially viable reactions are scarce and only the production of urea, salicylic acid, and carbonates have reached

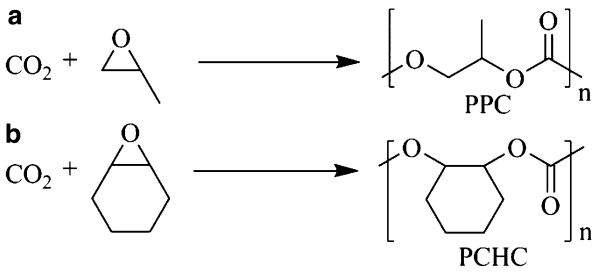

Fig. 7.1 Alternating copolymerization of propylene oxide (PO) (**a**) and cyclohexene oxide (CHO) (**b**) with CO_2

larger volumes [6, 7]. The amount of carbon dioxide consumed by these or any other chemical processes however cannot counteract anthropologically caused climate change. They rather have the potential to supplant oil-based starting materials in various synthetic pathways and thereby open up a more eco-friendly synthesis. The production of biodegradable polycarbonates from CO_2 and epoxides is currently receiving a lot of attention [5, 8, 9]. Aside from the polymeric product, cyclic carbonates also have potential applications such as in lithium ion batteries as electrolytes and as intermediates for the synthesis of linear dialkyl carbonates [4]. In this chapter cyclic carbonates will not be discussed in detail [9–11]. The focus will instead be on the catalysis behind the synthesis of polymeric materials with the recent developments at the center. Polycarbonates such as poly(propylene carbonate) (PPC) and poly(cyclohexene carbonate) (PCHC) have promising physical properties like lightness, durability, biodegradability, heat resistance, high transparency, and gas permeability which make them possible candidates for applications in the automotive, medical, and electronics industries.

7.2.1 Properties of Polycarbonates on the Example of Poly(propylene carbonate)

A large variety of epoxides are commercially available and subsequently have been tested for their behavior in copolymerization with carbon dioxide or even in terpolymerization with an additional epoxide. In industry though only ethylene oxide and propylene oxide are currently produced on large scale and have therefore a commercial advantage. Terpolymerizations promise a synthetic approach toward materials with better physical and material properties. Poly (propylene carbonate) and poly(cyclohexene carbonate) do not yet meet the demands of industry in respect of their glass transition temperatures, achieved molecular weights, elasticity, and their homogeneity. This justifies an academic approach toward better understanding of the polymerization behavior and properties of the produced materials.

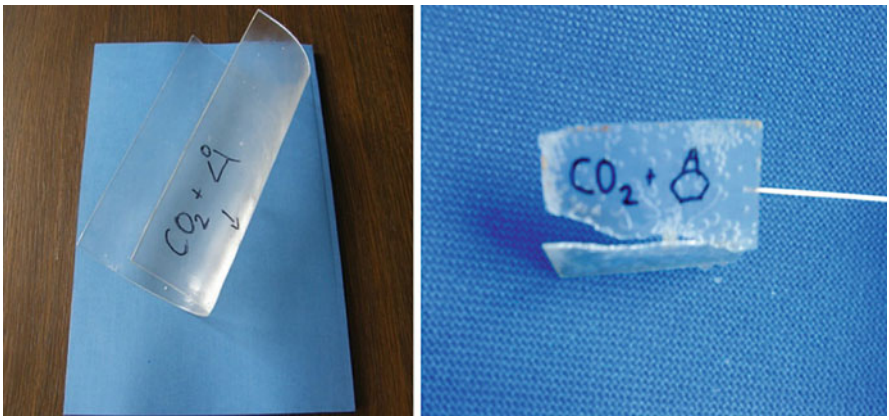

Fig. 7.2 Poly(propylene carbonate) (*left*), poly(cyclohexene carbonate) (*right*)

7.2.1.1 General Properties

Poly(propylene carbonate) is an aliphatic polycarbonate (Fig. 7.2). Due to irregular incorporation of carbon dioxide, polyether units can be presented in the polymer backbone. PPC is amorphous, hydrophobic, and soluble in organic solvents, e.g., dichloromethane, acetone, and cyclic propylene carbonate. The general properties strongly depend on the molecular weight, polydispersity, ratio of carbonate to ether linkages, microstructure, and possible catalyst contaminations in the polymer [12, 13]. Due to all the mentioned factors in literature, a temperature range from 25 to 46 °C for the glass transition temperature of PPC is given, and also other material characteristics like tensile strength and Young's modulus also show some variance [14, 15]. Cyclic carbonates act as plasticizers in the polymer and have the same effect as ether units in the polymer backbone: they decrease the glass transition temperature. Additionally, high amounts of ether linkages affect the material's thermal stability.

As the available analytical data is not always sufficient to correctly compare the investigated polymer samples, some properties only can be given as approximate ranges. For polymer samples with a T_g of about 40 °C, the range for the modulus was from 700 to 1,400 MPa, whereas for PPC with a T_g of 30 °C the modulus was reported to be 200 and 1,000 MPa [14, 15]. However, for strictly alternating PPC with less than 1 % cyclic carbonate content, an elongation at break of less than 50 % and a tensile strength of around 40 MPa (M_n = 180,000 g/mol) is reported in the literature [8]. One of the major disadvantages of PPC is its tendency to degrade at elevated temperatures. Earlier reports tested PPC with different molecular weights at temperatures between 150 and 180 °C. They observed severe degradation which of course has negative consequences for the material properties. Current publications suggest that the degradation is not solely induced by temperature, but that residual catalyst can enhance the degradation as well [16–20]. Already at 150 °C, a

PPC sample with a molecular mass over 200 kg/mol and a PDI of 1.2 show severe degradation to cyclic carbonate after 1 h if the catalyst residue is not completely removed from the polymer [12]. An increase in thermostability to 180 °C was made possible by a thorough catalyst removal from the sample. Further increases in temperature resulted in profound degradation even for the treated polymer sample. Blending of PPC with other engineering plastics is possible but difficult due to the fact that the optimum melt processing temperature for PPC is around 100–140 °C [21]. In general, polyesters and polyamides exhibit higher melting temperatures of above 200 °C [16]. The catalysts known in the literature so far show low productivity and produce at most 38 kg polymer per gram cobalt catalyst [22]. The catalysts cannot be left in the polymer due to their coloring- and degradation-enhancing properties. Furthermore, regulations concerning the amount of toxic metals like cobalt make a thorough clean up of the polycarbonates necessary.

7.2.1.2 Degradation Mechanism and Thermal Stability

In the previous subchapter, the thermal degradation of PPC was briefly addressed. Now the underlying mechanisms and possibilities for the formation of more stable PPC shall be discussed in more detail.

One form of thermal degradation is chain unzipping, whereby the nucleophile for the degradation can be located in the polymer chain or through an external nucleophile from another chain (Fig. 7.3a). Terminal hydroxyl groups can perform intramolecular backbiting reactions and thereby cause the formation of cyclic carbonates. The backbiting reaction can occur via a terminal alkoxide chain end which attacks at a carbonyl carbon. The backbiting route can also be via a terminal carbonate which attacks at an electrophilic carbon in the polymer chain. Intermolecular back biting leads to an attack at a random position in the polymer and forms shorter chains. The second degradation mechanism, which is assumed to take place increasingly at higher temperatures, is random chain scission (Fig. 7.3b) [23, 24]. At elevated temperatures, a decarboxylation reaction takes place and gives rise to carbon dioxide and an olefin moiety. As can be seen in Fig. 7.3c, catalyst impurities, water residues, acids, bases, and solvents promote degradation reactions and should therefore be thoroughly excluded or removed upon completion of the reaction [16].

The thermal stabilities reported in the literature are difficult to compare and to relate to one another due to a lack of information concerning both the polycarbonates and the testing conditions. Generally, the chain unzipping of poly (propylene carbonate) and other carbonates can be suppressed to a certain degree by end-capping, although the potential for depolymerization via chain scission is not affected by this alteration. In the end-capping process, the nucleophilic terminal hydroxyl groups of the poly(alkylene carbonates) are replaced with less reactive functionalities (e.g., isocyanates, carboxylic acid anhydrates, acetates, urethanes, sulfonates, phosphorous containing compounds) [23–27]. Analytical data concerning the remaining hydroxyl groups have not been published so far.

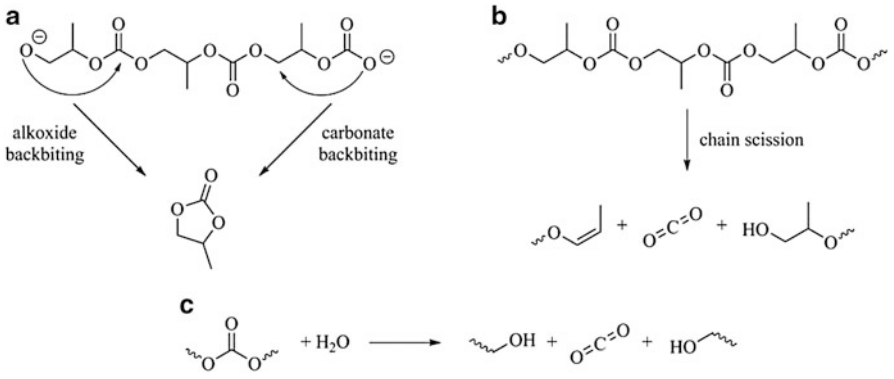

Fig. 7.3 Backbiting mechanisms for poly(propylene carbonate): (**a**) chain unzipping, (**b**) chain scission, and (**c**) residual water traces promoting the degradation

Hydrogen bonding has also been shown to improve the thermal stability of polycarbonates significantly. In a recent publication, octadecanoic acid was added to PPC by solution mixing. The resulting supramolecular complexes showed improved thermal stability, a thermotropic liquid crystalline character, and enhanced glass transition compared to an amorphous PPC copolymer [28]. Improvements in thermal stability were also obtained by adding wood flour [29] or nanoparticles [30–33] to polycarbonates by blending with other polymers [34–37].

The actual measured thermal stabilities are difficult to compare due to different testing conditions and the lack of information concerning the poly(propylene carbonates) themselves. It was reported that interactions between poly(propylene carbonate) and metal ions can in fact enhance the thermal stability [38–40]. Nevertheless, none of the modifications to poly(propylene carbonate) mentioned in the literature are able to inhibit degradation during processing at temperatures over 180 °C.

7.2.1.3 Terpolymerization

Terpolymerizations and block copolymerizations have the potential to overcome the poor properties of poly(propylene carbonate) and poly(cyclohexene oxide), respectively, and instead combine their strengths in one polymeric material. Other epoxides such as styrene oxide and epichlorohydrin offer additional opportunities as copolymers and also as substitutes for PO or CHO. Consequently, both the copolymerization and the terpolymerization of carbon dioxide and various epoxides have been investigated (Fig. 7.4) [41–54]. The incorporation of other monomers (lactones and anhydrides) in polycarbonate structures has also been studied [55–62].

Fundamental research on the reasons for the differing reactivities and on the inactivity of some catalysts toward some monomers is scarce. Rieger et al. published detailed kinetic studies supported by quantum chemical calculations in 2011 [63]. The homogeneous dinuclear zinc catalyst **26** of Williams et al. was chosen as a test system

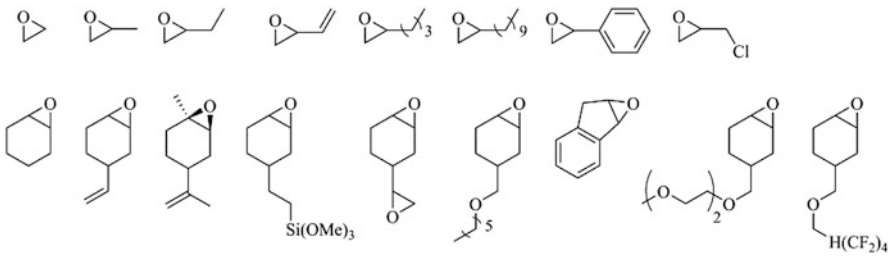

Fig. 7.4 Some epoxides used in the literature [41–54]

as it exhibits the highest activities for CHO/CO_2 copolymerization at one bar carbon dioxide pressure (TOF = 25 h^{-1}) [64]. The copolymerization of propylene oxide and carbon dioxide however is not possible with catalyst **26**: instead, only cyclic carbonate is formed. Many zinc-based catalyst systems share this inactivity for PO/CO_2 copolymerization or possess only low activities compared to other metals. Therefore, Rieger et al. systematically varied the reaction conditions to identify the underlying principles. They found that neither propylene oxide nor additionally added cyclic propylene carbonate does deactivate the catalyst for the formation of PCHC, although in the presence of cyclic propylene carbonate, the activity was decreased dramatically. Terpolymerizations with different ratios of CHO to PO resulted only in PCHC and no incorporation of PO was found, which can be attributed to a very fast backbiting reaction in the case of PO. DFT calculations showed that the ring strains of CHO and PO are comparable and that kinetic barriers to polymer formation in theory favor generation of PPC over PCHC. Consequently, the authors concluded that in the case of the studied zinc catalyst, the depolymerization rate of PPC is several magnitudes faster than that of PCHC. The limitations of zinc complexes gave cobalt catalysts an advantage in the field of CHO/PO and CO_2 terpolymerizations. In 2006 the first (salen)CoX catalysts with increased activities were discovered [46]. Catalyst **1**, in combination with [PPN]Cl, is able to terpolymerize at 25 °C and 15 bar CO_2 pressure equimolar quantities of PO and CHO with activities up to 129 h^{-1}. The resulting polymer had a narrow PDI of 1.24 and a high content of carbonate linkages and showed a single T_g. The authors varied the reaction conditions and were able to tune the CHO content from 30 to 60 % which gave polymers with T_g in the range of 50–100 °C. The highly alternating nature of the polymer was attributed to the inhibiting nature of CHO on PO which leaves both epoxides with matched reactivities in the copolymerization. The regioselective ring opening of PO was not disturbed by the competing binding of the epoxides to the metal center. Another cobalt-based catalyst (**7**) with covalently bound ionic groups was published in 2010 by Lee et al. They performed a multitude of experiments with various epoxides in different combinations [65]. Terpolymerizations of CO_2/PO/CHO, CO_2/PO/1-hexene oxide (HO), and CO_2/PO/1-butene oxide (BO) were carried out. Activities ranged between 4,400 and 14,000 h^{-1} and no cyclic carbonate formation was observed during the reactions. Furthermore, an increase in decomposition temperature was achieved by employing a third monomer and the results demonstrated that the T_g of PO/CO_2 can be

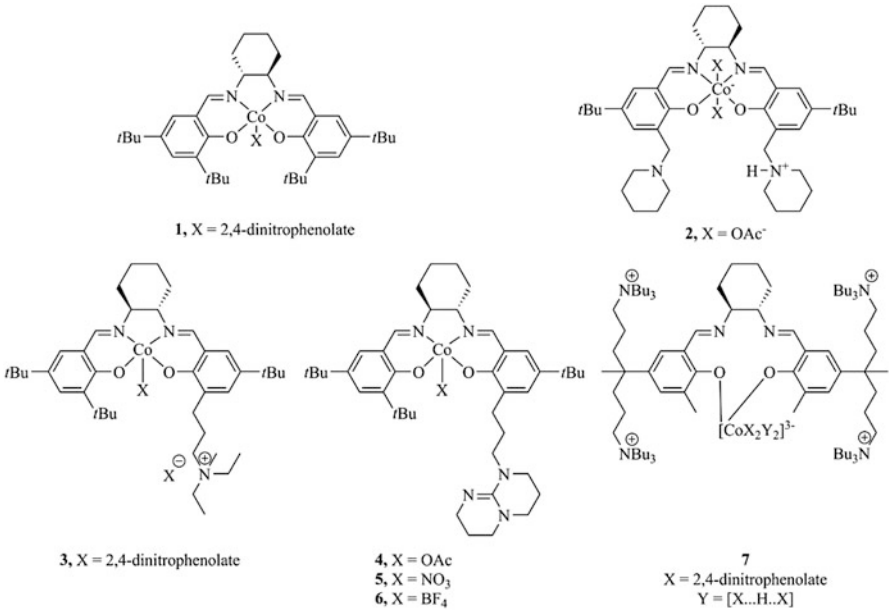

Fig. 7.5 Cobalt catalysts for the co- and terpolymerization of carbon dioxide and epoxides [22, 46, 65–67]

adjusted at will in a certain range (0–100 °C) by using a third monomer (CHO, HO, or BO). A linear dependency between the glass transition temperature in the terpolymer and the proportions of the third monomer was observed, which makes T_g adjustments possible. For the terpolymer CO_2/PO/HO, the temperature range was found to be from −15 to 32 °C and for CO_2/PO/BO from 9 to 33 °C. The authors also report that the incorporation of further epoxides (styrene oxide (SO), isobutylene oxide (IO), and glycidyl ether (GE)) in the PO/CO_2 copolymer failed under the tested reaction conditions due to remaining impurities in the monomers. Almost at the same time Lu et al. reported a bifunctional cobalt(III) catalyst (**3**) for the copolymerization of CHO/CO_2 and for terpolymerization with additional aliphatic epoxides such as PO, EO, BO, and HO (Fig. 7.5) [66].

The catalyst showed high activities (TOF) of 1,958–3,560 h^{-1} (90 °C, 25 bar, 1:1 = CHO: [PO,BO,HO,EO]) and molecular weights of the resulting terpolymers ranged between 40,000 and 60,000 g/mol (PDI ~ 1.1). The produced polymers had a content of 37–65 % of cyclohexene carbonate linkages and only one T_g was measured (32–79 °C).

Functionalized epoxides open up the possibility for post modification of the resulting carbonate structures. Already in 2007 Coates et al. used β-diiminate zinc(II) acetate catalysts ([(BDI)ZnOAc]$_2$) for the terpolymerization of CHO, vinylcyclohexene oxide (VCHO), and carbon dioxide to synthesize vinyl-functionalized polycarbonates [43]. The subsequent olefin metathesis using a Grubbs' catalyst [68] made the transformation of linear polycarbonates into nanoparticles of controlled size possible. The

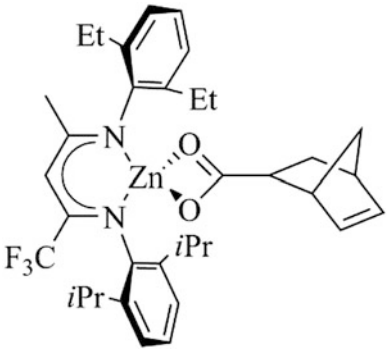

Fig. 7.6 BDI zinc catalyst with a norbornene carboxylate initiator [69]

employed epoxides had comparable reactivities, which enabled the generation of terpolymers with a VCHO content of 30 mol%. Medium molecular weights of 54,100 g/mol and low PDI ($M_w/M_n = 1.20$) were reached. It was observed that the cross-metathesis reaction progressed quickly in the beginning, but due to the formation of increasingly rigid polymer chains slowed down after 15 min. A remarkable increase in the T_g was observed from 114 to 194 °C at 76 % cross-linking. This increase was attributed to reduced chain mobility. A similar approach was used by Coates et al. in 2012 for the synthesis of multisegmented graft polycarbonates [69]. Norbornenyl-terminated multiblock poly(cyclohexene carbonate)s were again synthesized using a BDI zinc catalyst **8** with a norbornene carboxylate initiator (Fig. 7.6). The living nature of the copolymerization allowed the step-by-step addition of functionalized CHO. This generated variable block sequences which could subsequently be transformed to segmented graft copolymers by ring-opening metathesis polymerization.

Propylene oxide derivatives in terpolymers can also be found in the literature. Frey et al. terpolymerized 1,2-isopropylidene glyceryl glycidyl ether (IGG), glycidyl methyl ether (GME), and carbon dioxide [70]. After the acidic removal of the protecting acetal groups, a polycarbonate poly((glyceryl glycerol)-co-(glycidyl methyl ether) carbonate) (P((GG-co-GME)C)) is received. The analysis of the polymeric material showed monomodal molecular weight distributions and PDIs between 2.5 and 3.3, although the molecular mass was comparably low (12,000–25,000 g/mol). The T_g of the unprotected polymer was 3–5 °C higher than those of the corresponding protected copolymers. Interestingly, during investigations of the degradation behavior of the P((GG-co-GME)C) copolymers in THF solution, no backbone degradation was observed over 21 days. The authors ascribe this observation to the reduced stability of the resulting cyclic carbonate structures.

As can be seen in this chapter, the possibilities for further research are far from exhausted. Apart from the synthesis of ever more refined structures, the analytics must evolve simultaneously to access the microstructure. Therefore, current developments in the field of polymer NMR techniques will be discussed in detail in the next chapter.

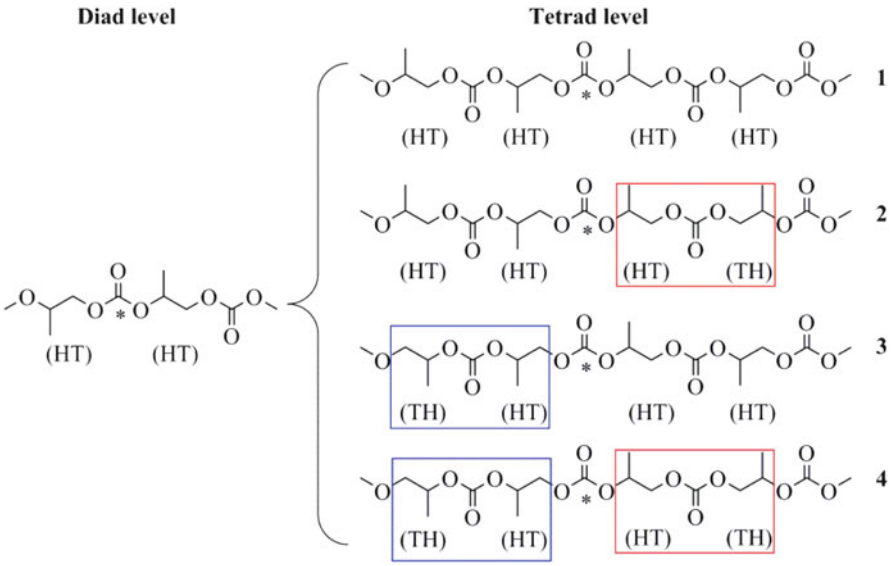

Fig. 7.7 *The four proposed* regiosequences with central HT junctions

7.2.1.4 Microstructure of Poly(propylene carbonate)

Since its first discovery, poly(propylene carbonate) has been characterized via a multiple analytical methods by various research groups [71–76]. NMR has been used extensively for microstructure analysis because PPC with higher stereoregularity has the potential to increase the glass transition temperature (T_g). In general, the ring opening of PO occurs via an S_N2 type mechanism at the methylene position resulting in a predominantly head-to-tail (HT) regiostructure of the CO_2/PO copolymer. By contrast, tail-to-tail (TT) or head-to-head (HH) connections arise if the ring opening of the epoxide takes place at the methine carbon. In 2002, Chisholm and colleagues assigned ^{13}C NMR spectra for different PPC copolymers using a statistical approach [17]. First, they studied the ^{13}C NMR spectrum of (*S*)-PPC obtained from the copolymerization of (*S*)-PO and CO_2 using a zinc glutarate catalyst. The carbonate carbon region showed more than one resonance, providing information about the possible regiosequences that occur at the tetrad level. Consequently, Chisholm et al. proposed four regiosequences with central head-to-tail (HT) junctions that are distinguishable by NMR for the carbonate carbons (Fig. 7.7).

The other carbonate carbon signals arising from TT and HH junctions at the diad level were assigned as *s*. Chisholm and colleagues applied the same statistical approach at the triad level for aliphatic carbon in PPC and later on they analyzed the structure of oligoether carbonates [17, 77]. Those compounds were potential models for the PPC microstructural assignments in NMR studies. It was possible to show with ^{13}C NMR investigations that the carbonate carbon signals have both

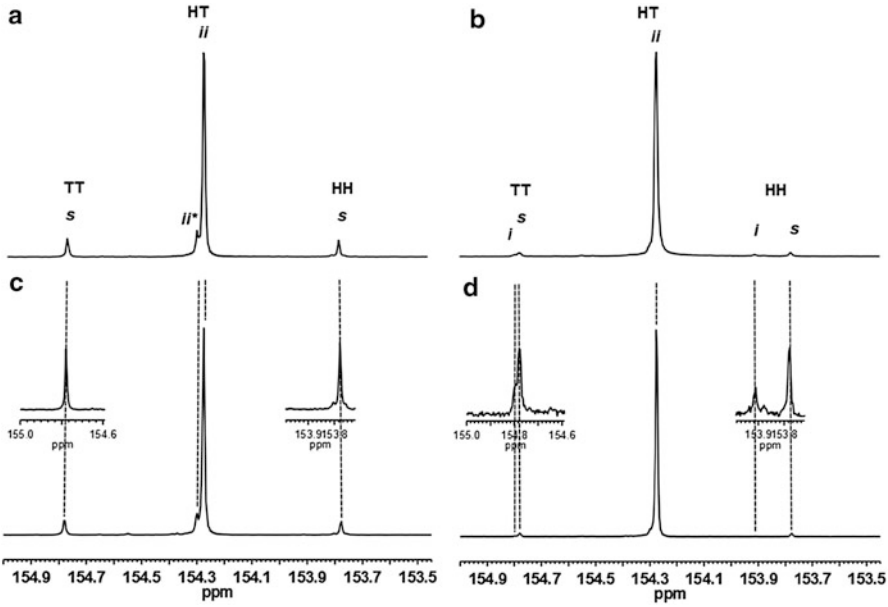

Fig. 7.8 ^{13}C (125 MHz, $CDCl_3$) NMR spectra (carbonate carbon region): (**a**) (*R*)-PPC copolymer, (**b**) (*R*)-PPC copolymer synthesized, (**c**) (*S*)-PPC copolymer, and (**d**) (*S*)-PPC copolymer, 1 equivalent [PPN]Cl, 1,000 eq. PO at 30 °C and 30 bar CO_2 for 20 h [(**a**) and (**d**) ((*R*,*R*)-(salen)CoCl) (**b**) and (**c**) (*S*,*S*)-(salen)CoCl] (Reprinted with permission from Ref. [78]. Copyright 2012, American Chemical Society)

regio- and stereosensitivity at the diad and tetrad levels to their adjacent ether units [77]. Density functional theory calculations were applied to the tested oligoether carbonates. These calculations indicated that the carbonate groups exist predominantly in *cis-cis* geometries with more than one stable conformation for each molecule. In addition, the ^{13}C chemical shifts predicted in the calculations were sensitive to the conformations of the molecules and the configurations of the stereocenters in PO ring-opened units. Recently, different poly(propylene carbonate) (PPC) microstructures have been synthesized by Rieger et al. from the alternating copolymerization of CO_2 with propylene oxide (PO) using chiral cobalt and (salen)Cr catalysts [78, 79].

The model which was presented in the study of Rieger et al. was based on triad structure obtained from ^{13}C NMR spectroscopy (HT carbonyl region). The ^{13}C NMR spectra of selected poly(propylene carbonate) samples were recorded using a 900 MHz (^1H) spectrometer, showing a previously unreported fine splitting of the carbonate resonances. Utilization of enantiopure and enantio-enriched PO allowed to apply the approach of isolated stereoerrors in the predominantly isotactic polymer to assign in detail the observed signals due to the stereo- and regioirregularities (Fig. 7.8). This assignment was performed under consideration of the direction of the polymer chain. Additional GC-analysis of the hydrolyzed polymers has shown a

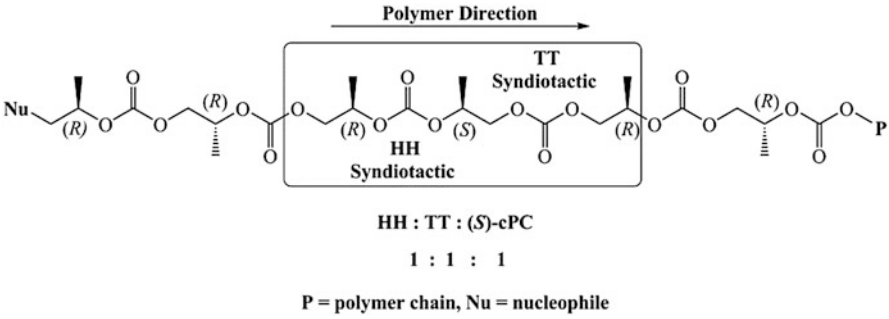

Fig. 7.9 Syndiotactic HH and TT in (*R*)-PPC synthesized using 1, resulting from "abnormal" epoxide ring opening at the methine position [78]

correlation between the extent of regioerror and the ring opening of PO with inversion of configuration at chiral atom, leading to *s*-HH diads. Signals of *i*-diads in the HH region were also observed in certain cases, which is referred to an "abnormal" PO-enchainment with retention of configuration of the stereocenters. The assignment of carbonate carbon signals at δ_C 153.8 and 154.8 ppm to HH and TT syndiotactic diads, respectively (Fig. 7.9), is consistent with the previous work of Chisholm and coworkers [80].

However, in the HT-region, a new low-intensity peak in the vicinity of the *ii*-signal at the lower field was observed, which could be assigned to an effect of an HH regioerror close to the isotactic triad. Accordingly, all observed low-intensity signals in the polymers with a lower isotacticity (δ_C 154.29, 154.30, 154.35, and 154.39 ppm) correlate well with the resonances in the HH region due to the regioerror (Fig. 7.10). Such correlation was also observed in case of the polymer with a predominantly syndiotactic structure, revealing a low-intensity peak at low field close to an *ss*-HT-signal.

Aside from the HT region, the splitting pattern of the signals in the HH region of the spectrum is informative with respect to the copolymer microstructure. The splitting of the signals in the TT region is not pronounced, therefore indicating a weak influence of the neighboring stereoconfiguration on the chemical shift of this junction. It is therefore expected that the HH junction has a stronger effect on chemical shifts in neighboring stereosequences than the TT sequence does.

In case of copolymers with a high extent of regioerrors, the described correlations are not so straightforward but still can be observed (Fig. 7.11). A greater number of peaks in the HT and HH regions are expected for such copolymers, where the model of isolated regioerrors is no longer valid.

Following the (S)-PO/(R)-PO ratios in the polymer chain during the rac-PO/CO_2 copolymerization reaction using GC and 500 MHz NMR spectroscopy provided insight into the understanding of the arising PPC microstructure. The suggested average microstructure of the copolymers shows a gradient change from *iso*-enriched to stereogradient microstructure with the polymerization time due to the catalyst enantioselectivity. Investigations by Nozaki et al. also led to the synthesis

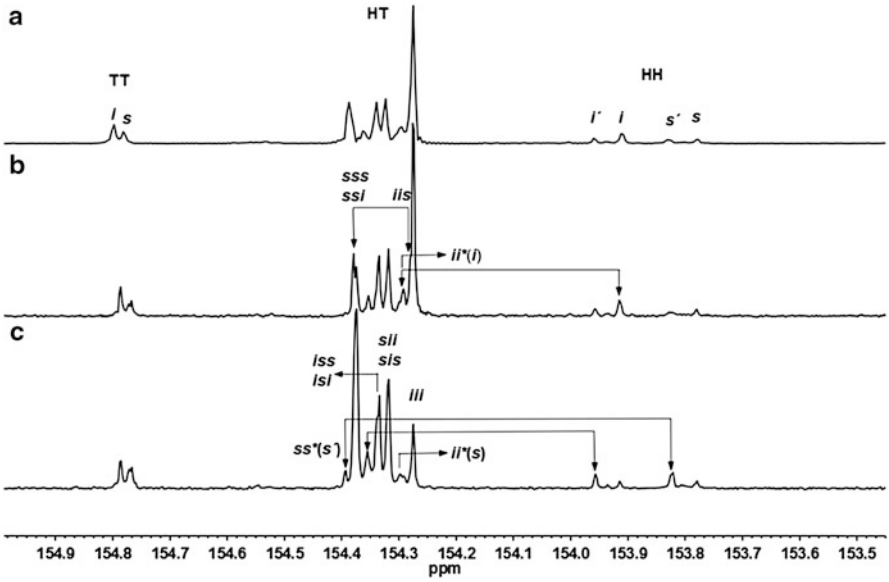

Fig. 7.10 ^{13}C NMR spectra of the carbonate carbon region of (**a**) *iso*-enriched PPC (125 MHz, $CDCl_3$), (**b**) *iso*-enriched PPC (225 MHz, $CDCl_3$), and (**c**) *syndio*-enriched PPC (225 MHz, $CDCl_3$) and the proposed assignment of signals on the tetrad level (Reprinted with permission from Ref. [78]. Copyright 2012, American Chemical Society)

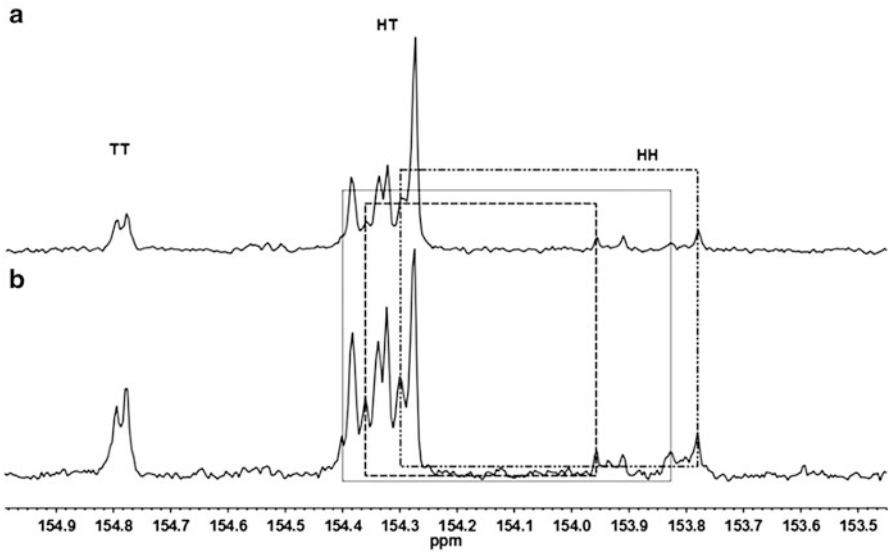

Fig. 7.11 ^{13}C (75 MHz, $CDCl_3$) NMR spectra for PPC copolymer synthesized using catalyst (salen)CrCl with 0.5 equivalent DMAP, (**a**) using 75 % (*S*)-PO and 25 % (*R*)-PO (**b**) using 25 % (*S*)-PO and 75 % (*R*)-PO at 50 °C and 50 bar CO_2 for 20 h (Reprinted with permission from Ref. [78]. Copyright 2012, American Chemical Society)

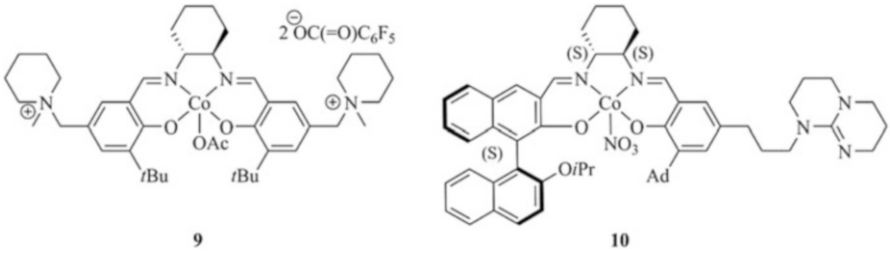

Fig. 7.12 (*left*) (salen)CoOAc **9** is capable of producing stereogradient PPC, (*right*) (salen)$CoNO_3$ **10** catalyst with pending TBD arm is capable of producing >99 % HT PPC [76, 81]

of stereogradient PPC which consisted of two enantiomeric structures on each end of the polymer chain [76]. The used catalyst was an optically active (salen)CoOAc with pendant ammonium arms. Thermal properties of the polymer were analyzed by differential scanning calorimetry (DSC) and thermogravimetry (TG).

Different regio- and stereoregularities did not show an influence on the glass transition temperatures ($T_g \sim 33$ °C) of the obtained polymers as was also confirmed by Rieger et al. [78]. But the stereogradient PPC and the stereoblock PPC exhibited higher thermal decomposition temperatures of up to 273 °C compared to PPCs with lower regio- and stereoregularities and iso-enriched PPC ($T_d = 240$ °C). The authors attributed their findings to a possible stereocomplex formation of a (S)-PPC block and (R)-PPC block in the same chain upon precipitation in methanol. Equimolar mixture of (S)-PPC and (R)-PPC did not show increased T_d values which might indicate a spatial dependence of the (S)-PPC and (R)-PPC for the stereoblock formation. Lu et al. achieved the synthesis of >99 % head-to-tail, >99 % carbonate linkage, and isotactic PPC with a multichiral (S,S,S)-(salen)$CoNO_3$ catalysts with a TBD group (1,5,7-triabicylco[4.4.0] dec-5-ene) anchored on the 5-position of one phenyl ring (Fig. 7.12) [81]. The isotactic PPC produced from (R)-PO exhibited elevated T_g values of up to 47 °C.

7.2.1.5 Microstructure of Poly(cyclohexene carbonate)

The copolymerization of *meso*-cyclohexene oxide and carbon dioxide produces poly(cyclohexene oxide) with different stereochemistry depending on the employed catalyst system. The ring opening of a meso-epoxide proceeds with inversion of the configuration at one of the two chiral centers (Fig. 7.13).

Nozaki et al. were the first to report asymmetric alternating copolymerization of *meso*-CHO with carbon dioxide. They used an equimolar mixture of Et_2Zn and (*S*)-diphenyl(pyrrolidin-2-yl)methanol as chiral catalyst [82]. Through alki-treatment, the PCHC was hydrolyzed into *trans*-1,2-diol and the degree of asymmetric induction was measured to be 70 % ee. These isotactic PCHCs were characterized via ^{13}C NMR spectroscopy using statistical methods and model compounds [83]. An

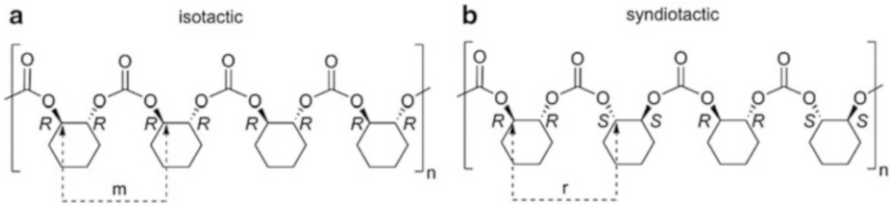

Fig. 7.13 Poly(cyclohexene oxide): isotactic (**a**) and syndiotactic (**b**)

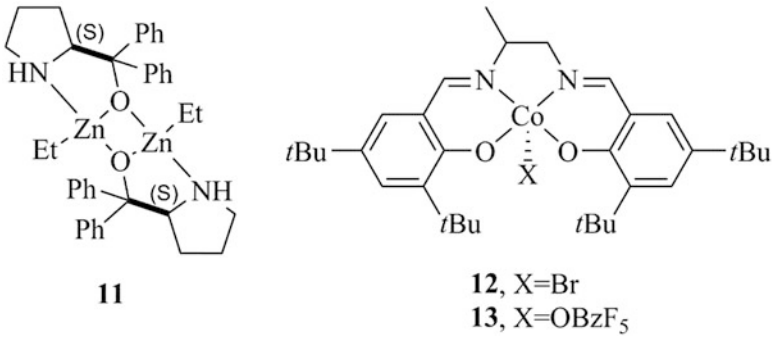

Fig. 7.14 Dinuclear zinc catalyst (**11**) (*left*), (salen)CoX catalyst (*right*) for the copolymerization of CHO and carbon dioxide [84, 85]

improved dimeric zinc system (**11**) was able to generate isotactic-enriched PCHC with 80 % ee [84]. End group analysis showed that the insertion of CO_2 happens at the zinc-ethoxy bond of the catalyst. Nevertheless, the obtained stereoregular copolymer (80 % ee) showed a T_g of 117 °C which is very close to that of non-stereoregular PCHC (115 °C) (Fig. 7.14).

The first syndiotactic-enriched PCHC was reported by Coates et al. who employed (salen)CoX catalysts for the copolymerization of CHO/CO_2 [85]. Catalyst (salen)CoBr (**12**) and (salen)CoOBzF_5 (**13**) were able to produce PCHC with up to 81 % r-centered tetrads. Through Bernoullian statistical methods, the PCHC triad and tetrad sequences were assigned in the ^{13}C NMR spectra in the carbonyl and methylene regions. The addition of cocatalyst ([PPN]Cl) resulted in the complete loss in syndiotacticity in the produced PCHC. The synthesis of enantiopure (salen)Co(III) catalysts (Fig. 7.15) by Lu et al. in 2012 made the synthesis of highly isotactic PCHC possible [86].

Chiral induction agents, such as (*S*)-2-methyltetrahydrofuran and (*S*)-propylene oxide, further improved the enantioselectivity regarding (*S*,*S*)-(salen)Co(III). PCHC with up to 98:2 *RR*:*SS* could be obtained with catalyst **1d**/[PPN]Cl in the presence of (*S*)-2-methyltetrahydrofuran. The highly isotactic PCHC was analyzed by DSC measurements and wide angle X-ray diffraction (WAXD). They found that PCHC samples with less than 90 % isotacticity did not show any crystallization.

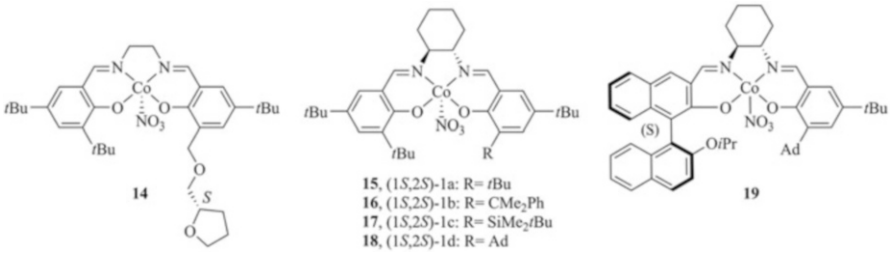

Fig. 7.15 Disymmetrical enantiopure (salen)Co(III) complexes[86]

(*R*)-PCHC with an *RR*:*SS* ratio of 92:8 ((*R*)-PCHC-92) gave a T_g of 122 °C and a small endothermic melting peak at 207 °C which stems from the low degree of crystallinity of the polymer. Contrary to amorphous PCHC, the (*R*)-PCHC-92 sample showed sharp diffraction peaks.

Aside from defined stereo- and regioregular synthesis of optical active PPC and PCHC, the catalytic side of the polymer formation has received much attention in recent years. The current development is refocusing on new possible ligand structures with less toxic metal centers which nevertheless can achieve high activities in the copolymerization. Those developments will be presented in the next section.

7.3 CO_2 Utilization in Polycarbonates

7.3.1 Development

Before diving into the broad field of polycarbonates and their synthesis and applications, a small review of historic developments is necessary to place the subsequent work in context. The earliest mention of the synthesis of poly(ethylene carbonate) was made in a patent in 1966 by Stevens [87]. However, it was not until 1969 that Inoue et al. presented their findings concerning the activity of a $ZnEt_2$/water mixture which was able to catalyze the formation of poly(propylene carbonate) from carbon dioxide and propylene oxide [73]. At pressures ranging from 20 to 50 bar and at 80 °C, the heterogeneous catalyst produced low molecular weight carbonates with turnover frequencies up to 0.12 h^{-1} and sparked a surge in developments over the next decades. In heterogeneous catalysis, Soga et al. synthesized the first well-defined catalyst system from a $Zn(OH)_2$/glutaric acid mixture, which is still the most active zinc-based system for copolymerization of CO_2 and propylene oxide [88]. By using different zinc carboxylates, Rieger et al. demonstrated the importance of the distance of the active zinc centers for catalytic activity. Problems arose in the evaluation of the active zinc centers, as well as the importance of crystallinity, surface, and particle size for this catalysis [10]. Furthermore, deeper understanding of the reaction mechanism was hampered by the drawbacks of heterogeneous catalysts in general. It is very

challenging to define the active sites in such systems and subsequently to ascribe structural alterations to activity increases or decreases. Furthermore, the multitude of active sites in the catalysts leads to broad polydispersity indices (PDI) which makes the characterization of physical properties of the polymer difficult. Consequently, it was not until 1978 that Inoue et al. published the first homogeneous catalyst system for the copolymerization reaction of CO_2 and epoxides [89]. The aluminum tetraphenylporphyrin complexes in combination with $EtPh_3PBr$ as cocatalyst were able to copolymerize not only cyclohexene oxide (CHO) but also propylene oxide (PO) with low PDIs. In 1995, *bis*(phenoxide)$Zn(THF)_2$ catalysts were synthesized and employed in the copolymerization of PO and also CHO and CO_2 [47, 90]. This catalyst system exhibited rather low activities and selectivities toward polycarbonate formation. The next important step toward well-defined and tunable catalysts was made by Coates et al. with the development of zinc β-diiminate complexes ((β-diiminate)ZnOR) [91]. This type of ligand allowed adjustment of the steric and electronic environment around the metal center and even small variations in the ligand framework already had drastic influences on activity and selectivity. Recently, Rieger et al. published a new dinuclear zinc catalyst system for the copolymerization of cyclohexene oxide and carbon dioxide. The catalyst **35** limits – in a certain broad pressure regime – the polymerization rate as a function of the applied CO_2 pressure. It is the first time that the rate determining step is shifted toward CO_2 insertion. This unique behavior is attributed to a flexible CH_2-tether that links both complex moieties. As a result, the highest known polymerization activities for CHO-based polycarbonates are reported.

Nowadays, development of these well-defined homogeneous catalysts and research on polycarbonates from carbon dioxide and epoxides are flourishing. Various review articles have been published in recent years in this field of research which demonstrates the growing interest in this material and the underlying mechanism [5, 9, 88, 92–97].

7.3.2 Mechanistic Aspects of the Epoxide and Carbon Dioxide Copolymerization

Homogeneous catalysts with the general structure L_nMX possess the great advantage of having only one defined active site. Tailoring the organic ligand L_n as well as the initiating group and the metal center provides a broad range of possibilities. Nevertheless, mechanistic investigations so far have not provided an unambiguous picture of the copolymerization of carbon dioxide and epoxides. Hence, three different possible reaction pathways shall be presented for a model salen complex.

The reaction pathway A requires interactions between two catalyst molecules and their active sites (Fig. 7.16). Thus, this mechanism is probable in the absence of a cocatalyst at low epoxide to catalyst loadings. It is rate dependent on the Lewis acidity of the corresponding metal center and on the nucleophilicity of the axial ligand X.

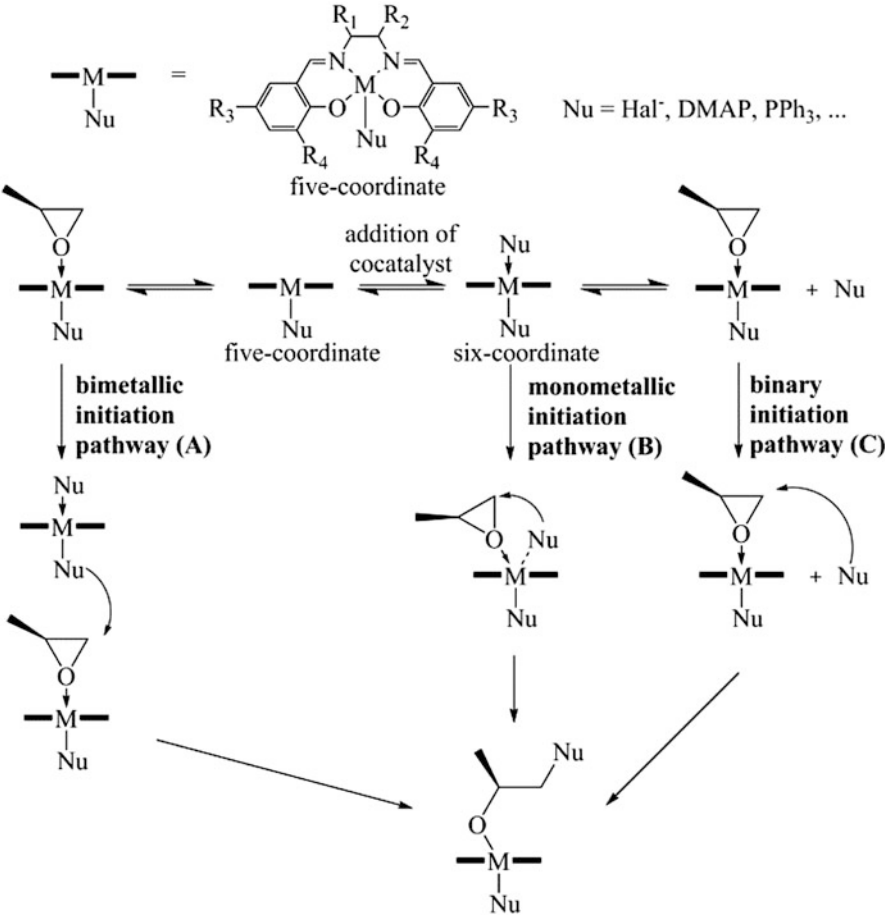

Fig. 7.16 Initiation mechanism for L_nMX for the copolymerization of carbon dioxide and PO: bimetallic pathway (**a**), monometallic pathway (**b**), and binary pathway (**c**) (Reprinted with permission from Ref. [88]. Copyright 2011, Elsevier)

Accordingly, the type of catalytic system used defines the mechanism. In the work of Jacobsen on the asymmetric nucleophilic ring opening of epoxides by chiral (salen)CrX complexes, this intermolecular, bimetallic pathway is a vital step in the absence of a cocatalyst [98]. The group of Rieger et al. also performed theoretical calculations concerning the chain-growth mechanism during the copolymerization of CO_2 and epoxides. The DFT calculations indicated that chain growth proceeds through the attack of a metal-bound alkyl carbonate on a precoordinated epoxide on a metal center [99]. However, other investigations indicated a bimetallic initiation step and subsequent monometallic chain propagation [71, 100–102]. Reaction pathway B is the monometallic mechanism and is comparable to an associative ligand exchange mechanism. In this scenario, the nucleophile and the epoxide are both bound to one metal center.

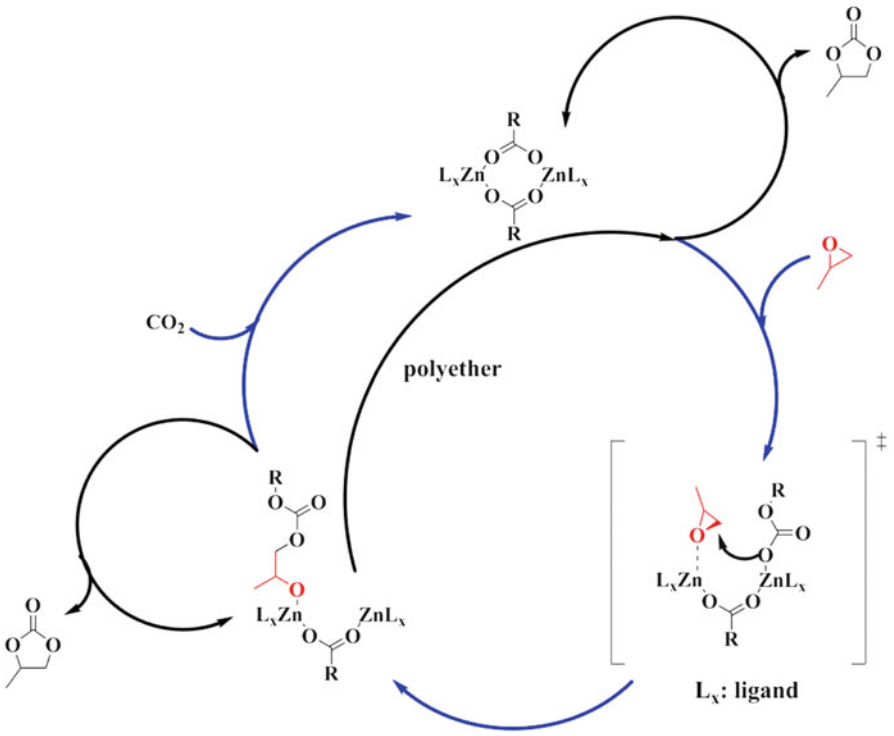

Fig. 7.17 Bimetallic propagation and the possible concomitant side reactions

In general, the epoxide is opened at the least hindered C-O bond but regioerrors may occur. Both the axial ligand and the nucleophile have the potential to open the epoxide and are therefore incorporated in the polymer chain as end groups. The thermally disfavored transition state makes this reaction mechanism unlikely for commonly used catalysts. Reaction pathway C takes place in the case of binary catalyst/cocatalyst systems where the added nucleophile attacks the precoordinated epoxide and opens the ring. Binary catalyst/cocatalyst systems have been under scrutiny from multiple research teams around the world in recent times [46, 85, 103–116].

The group of Coates et al. was able to show with (β-diiminate)ZnOR catalysts that a bimetallic mechanism is at play during their reactions [117]. Furthermore, they were able to find the rate determining step as the incorporation of the epoxide. The weak nucleophilic nature of the carbonate end group makes a preactivation of the epoxide necessary. Therefore, Lewis acids in the form of cocatalysts or a second metal center have to be used. After the ring opening of the epoxide, CO_2 is inserted into the metal alkoxy bond, for which an open coordination site at the metal is not obligatory. This mechanism explains the generally observed loss of activity of cocatalyst systems at higher dilutions (Fig. 7.17).

Undesired side reactions during the copolymerization are the formation of cyclic carbonates and the formation of polyether segments. The group of Darensbourg

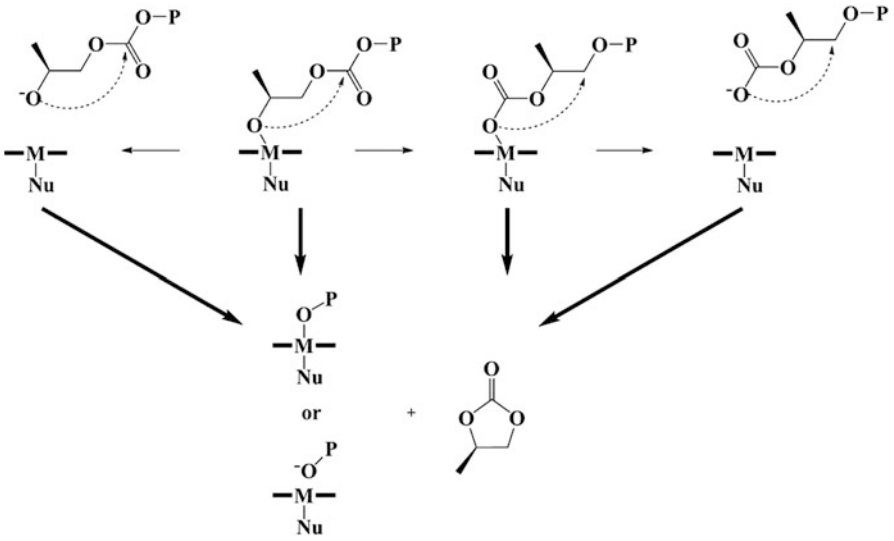

Fig. 7.18 Chain backbiting mechanism [88]

studied in detail the reasons for the product selectivity and the dependence on temperature, pressure, cocatalyst, and catalyst structure [101]. In general, both low temperatures and stronger coordination to the metal center decrease the amount of cyclic byproduct since these factors can suppress backbiting. During the backbiting reaction either the carbonato- or alkoxy-chain end of the polymer attacks at the growing chain (Fig. 7.18). This reaction is especially pronounced for aliphatic epoxides [63]. Alternatively, the growing chain end may dissociate from the metal center and more easily undergo backbiting in its unbound state [99]. The protonation of this unbound alkoxy- or carbonato-chain end is a possible strategy to reduce backbiting.

Chain transfer reactions during the copolymerization can be caused by traces of water, alcohols, or acids. Chain transfer can be exploited to tune the molecular weight by addition of, for example, adipic acid or telechelic polymers featuring alcohol end groups [118]. These chain transfer reactions lead to lower molecular weights than theoretically calculated. Furthermore, phosphoric acid and phenylphosphonic acids as additives have been tested to afford flame-retarding PPCs [42].

7.3.3 Catalysis

7.3.3.1 Bifunctional Catalysts

Owing to the desire to reach high selectivities and activities, catalyst design has shifted in recent years toward bifunctional catalysts. These complexes combine the

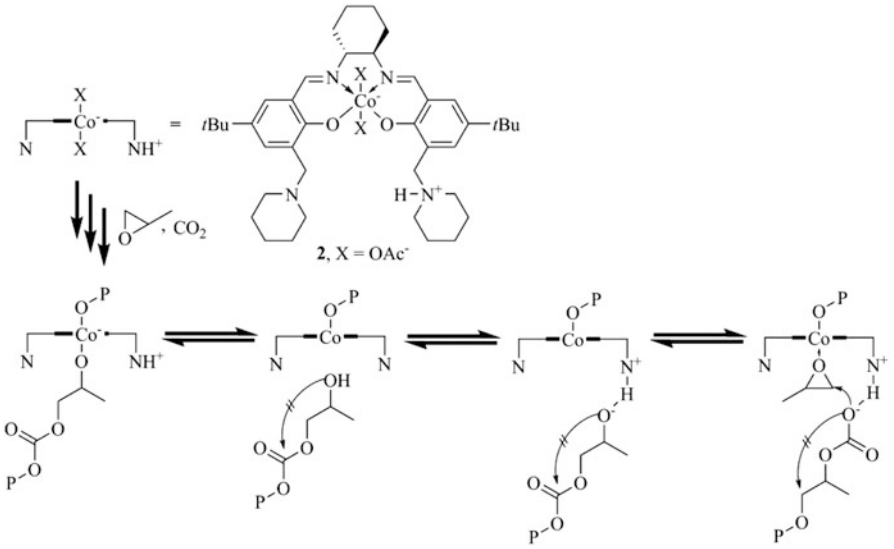

Fig. 7.19 Copolymerization mechanism for a bifunctional salenCo(III) complex with a piperidinium arm [67] (Reprinted with permission from Ref. [88]. Copyright 2011, Elsevier)

active metal site, coordinated by an organic ligand framework, with a covalently bound cocatalyst. With these considerations in mind Nozaki et al. incorporated a piperidinium arm into a (salen)CoOAc complex. It was proposed that cyclic carbonate formation is inhibited by the protonated piperidinium arm which can protonate the growing polymer chain upon dissociation from the metal center (Fig. 7.19). At a catalyst loading of PO/catalyst = 2,000, 14 bar and ambient temperatures, a selectivity of 99 % for poly(propylene carbonate) was achieved. Furthermore, it was shown that even at elevated temperatures of 60 °C, the cyclic carbonate formation could be suppressed to a certain degree [67].

The group of Lee et al. designed a series of ionic bifunctional catalyst structures in which the cocatalyst is covalently bound and is supposed to keep the growing polymer chain close to the reactive center [22, 119]. The anions also function as initiators for the copolymerization and have a pronounced effect on polymerization activity and product selectivity [120]. These catalysts were employed in copolymerization reactions with various epoxides, for example, cyclohexene oxide, hexene oxide, 1-butene oxide, and propylene oxide [48]. Polymerizations of PO and carbon dioxide at 80 °C and at dilutions as low as 0.67 mmol% were shown to be possible while retaining high activities and selectivities for the polycarbonate formation (TOF 12,400 h^{-1}, 96 %) [22]. The highest reported TOF is 26,000 h^{-1} (>99 %, M_n = 114 kg/mol, PDI = 1.29). It was possible to produce high molecular weight PPC at elevated temperatures with a M_n of up to 285 kg/mol and narrow molecular weight distributions of 1.18. Interestingly, the catalyst structure allowed the removal from the produced polymer after the copolymerization.

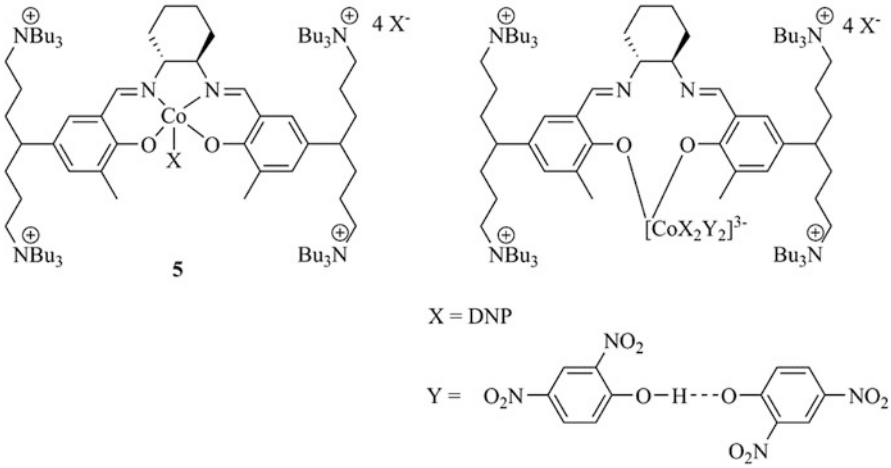

Fig. 7.20 Bifunctional ionic salenCo(III) catalyst **5** and its proposed bidentate coordination structure [121]

Filtration through a short pad of silica gel results in a catalyst which exhibits almost equivalent copolymerization activities even after several separation cycles. In their later work the group of Lee discovered an unusual coordination mode in their bifunctional catalysts. Though no crystal structure has yet been obtained from this proposed conformation, NMR studies and DFT calculations support the proposed structure. They postulated that the imine nitrogens of the salen ligand do not coordinate to the cobalt center (Fig. 7.20). Instead the DNPs coordinate to the cobalt, forming a negatively charged cobaltate complex. Structural variations of the ligand framework allowed the conclusion that sterically more demanding substituents in *ortho*-position reduce the activity. The authors attributed this to the fact that the formation of the aforementioned bidentate cobalt coordination is inhibited. High copolymerization activities were only observed on catalysts with the ability to form the cobaltate complex (Fig. 7.20 (right)) [121]. The employed 2,4-dinitrophenolate is explosive in its dry state as well as hazardous. Therefore, anion variations were performed using 2,4,5-trichlorophenolate, 4-nitrophenolate, 2,4-dichlorophenolate, and nitrate [118, 120]. It was found by chance that homoconjugated anion pairs of the phenols [X-H-Y] show increased activities and higher tolerance to water impurities leading to shorter induction periods [121]. Interestingly the rather long induction periods of the cobalt complexes during the copolymerization of epoxides and carbon dioxide are still unexplained. Further examples of bifunctional catalysts for the production of polycarbonates were published by Lu et al. These (salen)CoX complexes feature either an alkyl arm with pending quaternary ammonium salt at the 3-position of the phenyl ring or an alkyl arm bound to 1,5,7-triabicyclo[4,4,0] dec-5-ene (TBD). Catalyst **4** with the TBD group was able to polymerize with high selectivity for polycarbonate (97 %) at 100 °C and 20 bar. Activities up to 10,880 h^{-1} at a loading of 1 mmol% were

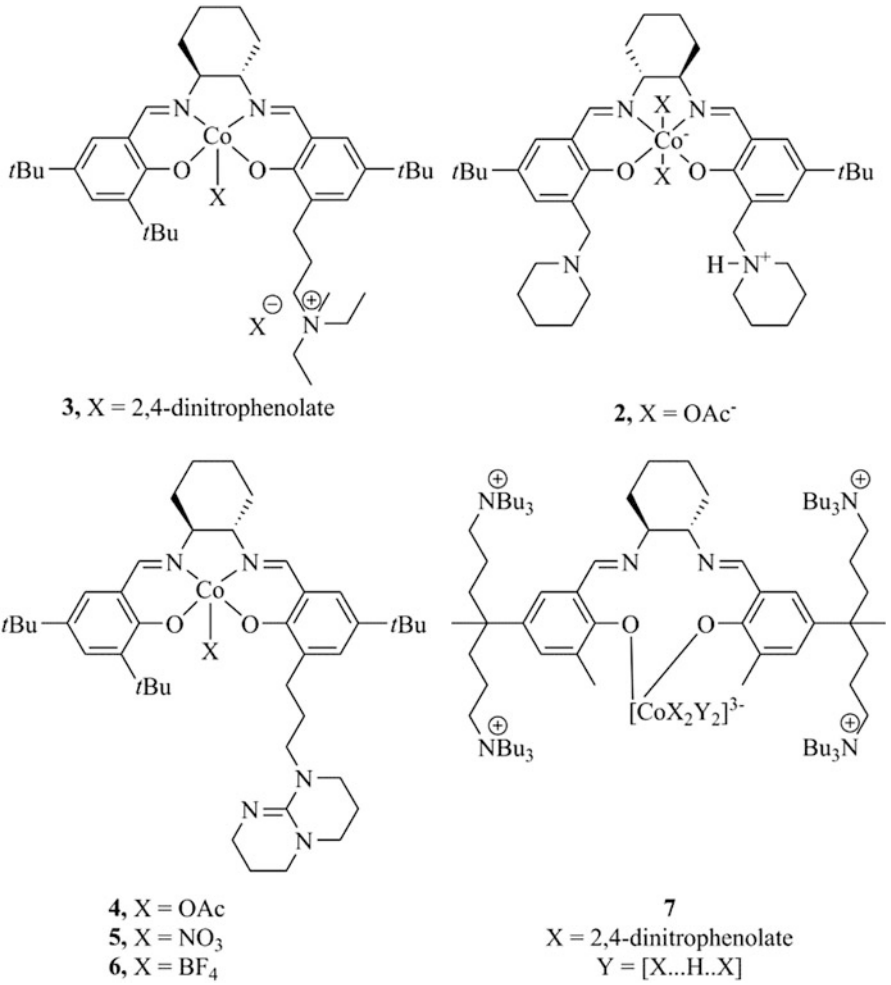

Fig. 7.21 Bifunctional salenCo(III) catalysts [22, 66, 67]

reached [122]. Through mass spectroscopy, it was possible to show that the pending TBD arm is activated after the insertion of one PO and carbon dioxide molecule. It stabilizes the Co(III) species against reduction to the inactive Co(II) by reversible intramolecular Co-O bond formation (Fig. 7.21).

The Co(III) catalyst (**3**) with an ammonium salt ($-NEt_2Me^+$) and 2,4-dinitrophenolate proved to be less active with TOF of 3,900 h^{-1} at 90 °C while nevertheless maintaining high selectivity for copolymer formation.

Bifunctional cobalt catalysts are currently the catalysts of choice for further scientific studies and improvements due to their excellent activities combined with high selectivities for the polymer formation. However, their main drawbacks cannot be solved by synthetic design as cobalt is toxic, prone to reduction, and has to be

removed from the polymer after copolymerization. This puts a considerable energetic burden on the produced polymer and hampers its chances to compete with already established polymers.

7.3.3.2 Zinc Catalysts

Due to their colorlessness, nontoxicity, and low price, it is not surprising that there is a considerable amount of literature on Zn(II)-based catalysts. For heterogeneous catalysis, the zinc glutarate (ZnGA) system is the most widely studied one. It is easy to prepare, nontoxic, economically viable, and easy to handle. But these heterogeneous catalysts are not only interesting for industrial applications as they offer the opportunity to better understand the reaction processes. The molecular structure of ZnGA was only recently reported and showed a unique structural constitution [123]. It consists of Zn centers coordinated by four carboxyl groups with the glutarate ligands either in a bent or an extended conformation. This structural type limits the activity for the copolymerization to the surface due to restricted monomer diffusion [124]. Consequently, methods for enlarging the surface were tested but with unsatisfactory results with respect to the achieved activity. Also the replacement of GA by derivatives (e.g., 2-ketoglutaric acid, 3,3-dimethylglutaric acid) with other functionalities in the hydrocarbon chain did not bring the expected success [125]. Experiments with different alkyl lengths (succinic acid (SA), adipic acid (AA), pimelic acid (PA)) in between the Zn centers showed that these are also active [126, 127]. It was not until 2011 that Rieger et al. published a detailed study of ZnSA, ZnGA, ZnAA, and ZnPA and their respective activities in the copolymerization of epoxides and CO_2 [128]. From the copolymerization experiments, the activity gap between ZnSA and the higher homologues was identified. The molecular structure was the crucial factor as the main difference between ZnSA and the tested homologues was the Zn-Zn distance. This indicated that the defined spatial structure which is influenced by the dicarboxylic acid has direct influence on the activity of heterogeneous zinc dicarboxylate systems. The Zn-Zn distance that is necessary for copolymerization is only found on one of the main *hkl*-indiced plains of the solid-state structure of ZnSA. However, in the solid-state structure of ZnGA, the corresponding distance of 4.6–4.8 Å is found on each main *hkl* plain (Fig. 7.22). These results show that two zinc centers have to be in close spatial proximity for high copolymerization activities to be possible. Theoretical calculations suggest that the optimal Zn-Zn distance for CO_2/epoxide copolymerization is between 4.3 and 5.0 Å [129].

This range gives an optimum between the activation energy and product selectivity toward polymer formation. The importance of the appropriate Zn-Zn distance for homogeneous catalysts was already described in literature. The study of Rieger et al. indicates that also in heterogeneous Zn catalysts a bimetallic mechanism is at play on the surface for which the spatial separation of the metal is crucial. To gain deeper insights into the copolymerization mechanism, homogeneous single-site

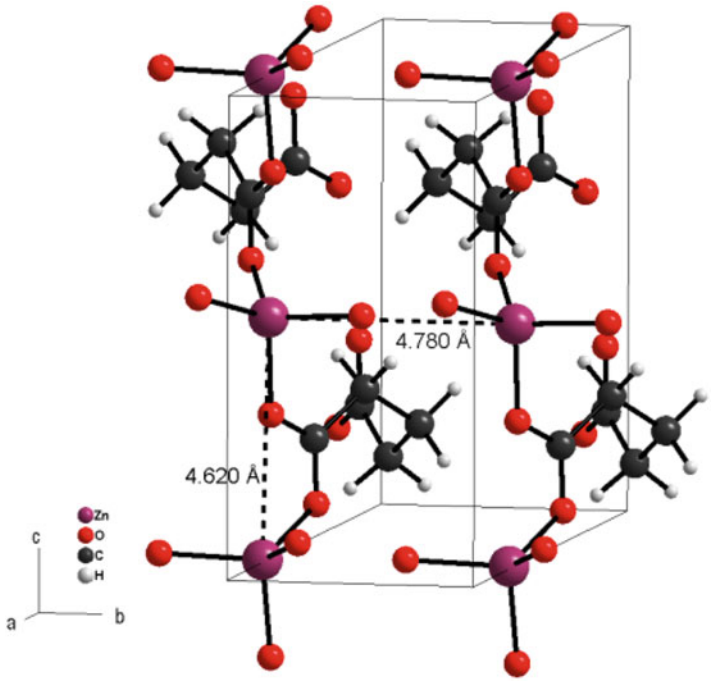

Fig. 7.22 Close-up view on unit cell and metal distances in zinc glutarate (Zn-Zn distance = 4.6-4.8 Å) (Reprinted with permission from Ref. [128]. Copyright 2011, American Chemical Society)

catalysts are required. Darensbourg et al. synthesized the first homogeneous zinc-based catalyst for the copolymerization of cyclohexene oxide and CO_2 [47]. These catalysts exhibited a strong tendency to form polyether even at elevated CO_2 pressures (55 bar). Major drawbacks of those early systems were the low activities and selectivities for polycarbonate formation. In the case of the phenoxide zinc complexes, another side reaction limited success as their phenoxide ligands were consumed as initiators during the polymerization [51, 130]. The unstable nature of the zinc phenoxide catalysts made mechanistic investigations and the defined synthesis of the ligand framework around the metal center difficult. The first breakthrough for copolymerization of epoxides and carbon dioxide was the discovery of β-diketiminato zinc catalysts (BDI) for the CHO/CO_2 copolymerization by Coates et al. which led to a more systematic catalyst design. Minor variations in the electronic and steric character of the BDI ligand framework resulted in dramatic changes in catalytic activity [47, 48]. These catalysts afforded polymers with narrow PDIs at low carbon dioxide pressures with high activities. In the copolymerization reaction of CHO/CO_2, minor changes in the backbone from R^1 = H, R^2, R^3 = Et to R^1 = CN, R^2 = Me and R^3 = *i*Pr led to an activity increase from 239 to 2,290 h^{-1} [91]. As shown in Fig. 7.23, these complexes are present in monomer/dimer equilibria which depend on sterics, electronics, and temperature.

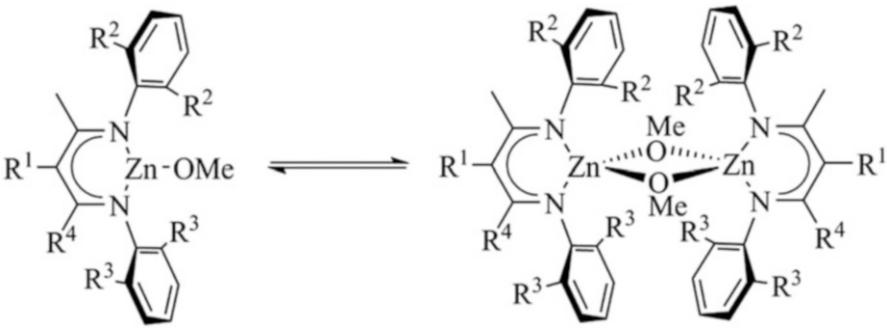

Fig. 7.23 Monomer/dimer equilibria for the zinc-based catalysts by Coates et al. [91]

Rate studies with in situ IR spectroscopy on the copolymerization resulted in a zero-order dependence in CO_2, a first-order dependence in CHO, and a varying dependency from 1.0 to 1.8 for zinc [117]. This variation can be constituted with the appearance of the mentioned equilibrium in Fig. 7.23. All results support the assumption that two zinc centers are interacting in the copolymerization and that the rate determining step is located at the ring opening of the epoxide. Additionally, it was found that sterical variation (R^1 = Et, R^2 = *i*Pr) at the aniline moiety and the introduction of electron withdrawing groups to the catalyst (**20**) backbone gave an active catalyst for the copolymerization of PO/CO_2 at 25 °C, 6.9 bar with a TOF of 235 h^{-1}. The resulting polymer featured a regioirregularity and a narrow molecular weight distribution [131] (Fig. 7.24).

Interestingly this complex structure also polymerized β-butyrolactone and β-valerolactone to afford atactic poly(3-hydroxybutyrate) (PHB) and poly (3-hydroxyvalerate) [132]. Research into the zinc BDI systems led to the discovery of ethylsulfinate as superior initiating group [133]. In 2005 Lee et al. presented an anilido-aldimine ligand for dinuclear zinc complexes (Fig. 7.25). Thereby, open (**22**) and closed (**21**–**24**) structures were synthesized with zinc-zinc distances of between 4.88 Å for the open structure and 4.69 Å for the closed structure. For the copolymerization of cyclohexene oxide and carbon dioxide, only the catalyst with the open structure was active. With this catalyst TOFs up to 200 h^{-1} were achieved. Increasing the Lewis acidity of the zinc centers led to an increase of activity up to 2,860 h^{-1} at high dilutions ([catalyst]:[CHO] = 1:50,000) [134, 135].

In 2011, Williams et al. published a rigid dinuclear zinc complex for low-pressure copolymerization of cyclohexene oxide and CO_2. Investigations of this catalyst system also revealed a zero-order dependence on CO_2 (between 1 and 40 bar CO_2 pressure) and a first-order dependence on CHO. These results confirmed the hypothesis that the incorporation of the epoxide is rate determining for their dinuclear rigid zinc catalysts [136]. This implies that at typical process conditions, an increase in CO_2 concentration does not automatically enhance polymerization activity. In subsequent work, Williams et al. replaced zinc with cobalt(II)/(III) [137] and iron [138] in the reduced Robson-type ligand structure (Fig. 7.26). The isolated complexes

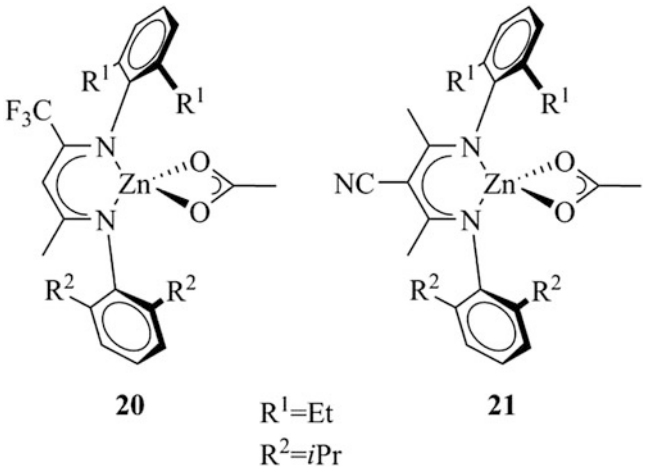

Fig. 7.24 Zinc catalyst for copolymerization of propylene oxide and carbon dioxide [131]

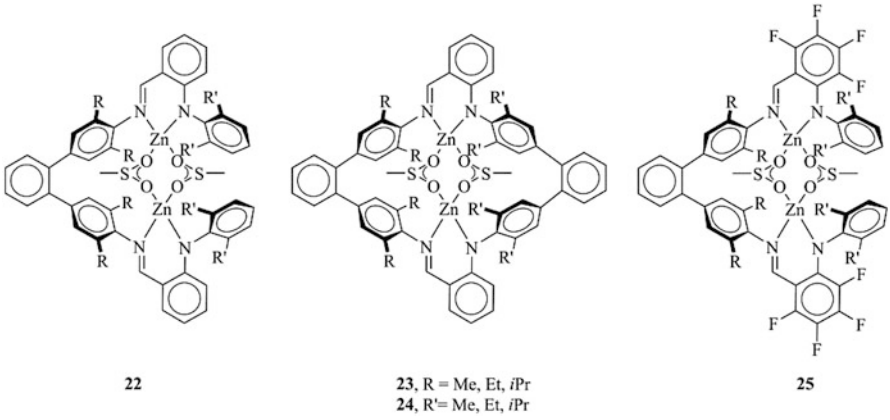

Fig. 7.25 Dinuclear anilido-aldimine zinc complexes [134, 135]

were all able to copolymerize CHO and carbon dioxide with good activities and high selectivities. The highest activities in the copolymerization of CHO and CO_2 were achieved with magnesium (**31**). Activities of up to 750 h^{-1} and very high selectivities of >99 % for the copolymer formation were observed with this structure (12 atm CO_2, [CHO]:[31] = 1:10,000, PDI = 1.03/1.10). The data gathered from these metal screenings show very nicely how the copolymerization activity can be tuned in dinuclear catalysts by the Lewis acidity of the metal itself.

In 2013, Rieger et al. presented a flexibly tethered dinuclear zinc complex **35**, in which two BDI zinc units are linked by a tether (Fig. 7.27). The linker allows to overcome the entropically disfavored aggregation of two individual complex molecules in solution. Catalyst **35** exhibits very high activities of up to 9,130 h^{-1} for the

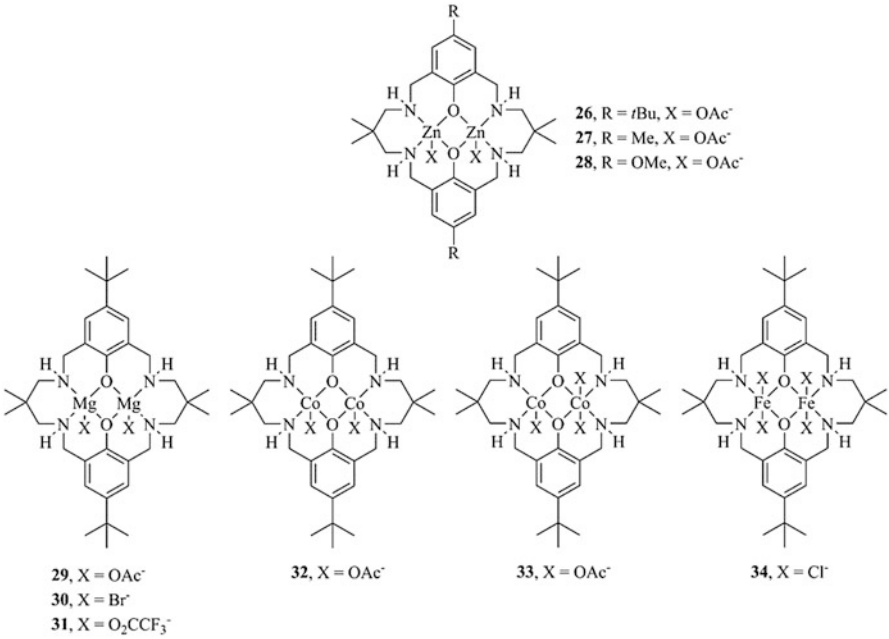

Fig. 7.26 Dinuclear reduced Robson-type complexes with Zn-, Mg-, Co-, and Fe-centers [64, 136–139]

Fig. 7.27 Flexibly tethered dinuclear zinc complex [140]

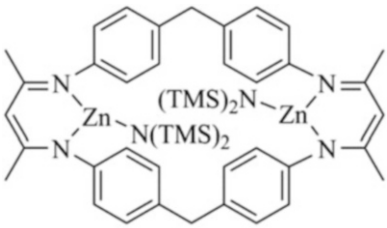

35

copolymerization of CHO and carbon dioxide (at 40 bar CO_2, 100 °C, [CHO]: [35] = 4,000:1) [140].

Kinetic measurements in an in situ IR reactor revealed a first-order dependence in catalyst. Interestingly, with constant catalyst and cyclohexene oxide concentration, the order in carbon dioxide was determined to be one in the range of 5–25 bar CO_2 pressure. For 25–45 bar, this order changes from one to zero. The assignment of the order in cyclohexene oxide was performed at two different pressure regimes: 10 and 30 bar, respectively. This resulted in a reaction order of zero for 10 bar and a reaction order of one at 30 bar. The subsequent rate laws are depicted below:

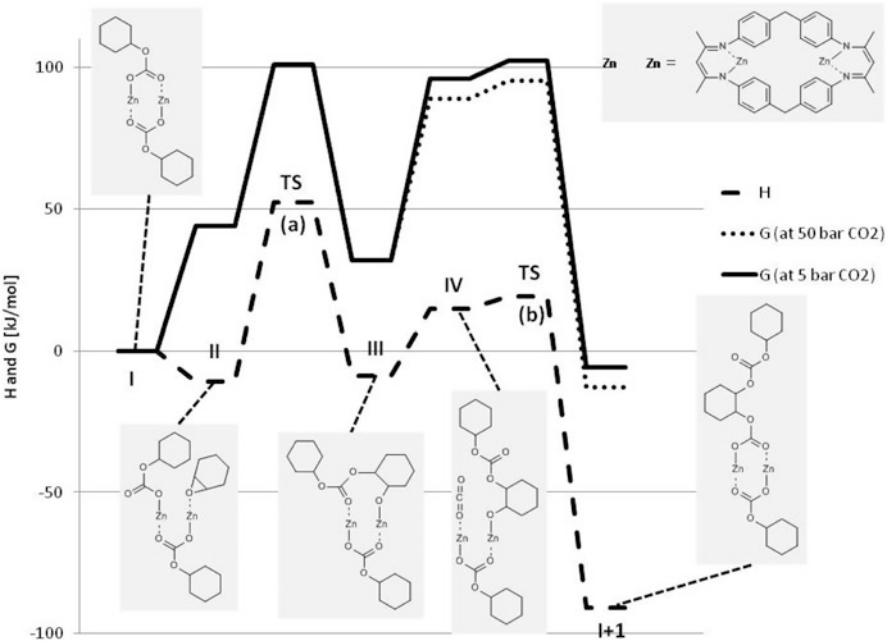

Fig. 7.28 Enthalpy and Gibbs free energy profile for the whole catalytic cycle of catalyst **35** (Reprinted with permission from Ref. [140]. Copyright 2013, Wiley-VCH Verlag GmbH & Co. KGaA)

Equation 7.1: Rate law of complex **35** for 5–25 bar CO_2 **(a)** and for 25–45 bar CO_2 **(b)** [140].

$$r = k \cdot [CHO]^0 \cdot [CO_2]^1 \cdot [Catalyst]^1 \quad 5-25 \text{ bar } CO_2 \quad (a)$$

$$r = k \cdot [CHO]^1 \cdot [CO_2]^0 \cdot [Catalyst]^1 \quad 25-45 \text{ bar } CO_2 \quad (b)$$

Catalyst **35** is the first dinuclear zinc catalyst which shows a shift in the rate determining step from ring opening of the epoxide to carbon dioxide insertion for the copolymerization of cyclohexene oxide and carbon dioxide in a certain pressure regime. This unique behavior is attributed to the flexible CH_2-tethers which links both complex moieties. Considering the first-order dependence with respect to CHO of all other catalysts, this suggests that the flexible tether between the two zinc centers facilitates the cooperative ring-opening step in an unprecedented manner. These results are supported by quantum chemical calculations. The computed results for the main steps, beginning from the dicarbonato complex as the starting point, followed by coordination of CHO, epoxide ring opening to form an alkoxide and subsequent insertion of CO_2 into the coordinated alkoxide bond, are summarized in Fig. 7.28.

As can be seen in Fig. 7.28, both elementary steps give similar computed G-values (~100 kJ/mol) which means that both transition states are equally difficult to overcome. It is notable that the enthalpy H is much bigger for the ring opening (TS (a) = 52.3 kJ/mol) compared to the H of the CO_2 insertion (TS(b) = 19.2 kJ/mol). At first glance, it appears surprising that elementary steps with such dissimilar activation energies can both be rate limiting. DFT calculations explain the similar activation energies as a consequence of Gibbs free energy which includes both activation enthalpy and entropy. The main point is that all alkoxide species are significantly higher in G if compared to the dicarbonato complex I, which is why all Gibbs free energies have to be considered in relation to complex I. As the resting state is in all cases the dicarbonato complex I, oxirane ring opening is a bimolecular reaction, i.e., the incorporation of one liquid species into the catalyst bound polymer chain. Otherwise, CO_2 insertion is effectively a trimolecular reaction, which consumes both one liquid epoxide and one gaseous CO_2. All the structural and electronic features of **35** lead to high copolymerization activities of over 9,130 h^{-1} and selectivities of >99 % toward polycarbonate formation.

In conclusion, zinc and other nontoxic, cheap, and abundant metals have tremendous advantages compared to other transition metals, namely, cobalt and chrome, which are currently predominantly employed for the copolymerization of carbon dioxide and epoxides. In recent publications, it was nicely shown how those economic and eco-friendly elements can achieve high activities and selectivities. An additional advantage of zinc and magnesium is their colorless ions. This opens up the possibility to leave the catalyst in the formed polymer and reduce work-up costs.

7.4 Conclusion

Carbon dioxide as feedstock for the generation of biodegradable polycarbonates has been known in the literature for almost 45 years. Since the discovery of the copolymerization reaction of carbon dioxide and epoxides, chemistry has made significant progress, and especially in the last 10 years, the search for better and more eco-friendly catalysts has gained momentum. As the stereoselective synthesis of poly(propylene carbonate) is still in its infancy and the analytical methods used have not yet been fully exploited, NMR techniques have the potential to help interpret the structures produced by catalyst systems and to pinpoint promising catalyst candidates for further development. Though heterogeneous catalysts still dominate industrial production processes, for mechanistic investigations, homogeneous systems do have the necessary advantages to tackle the underlying questions about the mechanism and within the catalysis. Cobalt(III) catalysts with a variety of accompanying ligand structures have become the center of attention since the discovery of bifunctional structures which allow the incorporation of the cocatalyst into the complex and thereby enable high activities and the production of polycarbonates with high molecular masses, low PDIs, and >99 % carbonate

content. However, cobalt as toxic and coloring metal has to be removed from the polymer after copolymerization. Any additional work-up increases the energetic burden on production and limits competitiveness of biodegradable polymers such as poly(propylene carbonate). Possible applications in food packaging also make the development of less toxic catalysts desirable. An applicable catalyst for large-scale industrial production in a continuous process has to exhibit a sufficient activity to make it economically viable. In recent years, research made great progress in the development of iron-, magnesium-, and zinc-based systems which show improved activities. It will be interesting and exciting to see the future development of catalyst systems which tolerate water contaminations and multiple epoxides and nevertheless show high activities in co- and terpolymerizations at ambient conditions.

References

1. Song C (2006) Global challenges and strategies for control, conversion and utilization of CO_2 for sustainable development involving energy, catalysis, adsorption and chemical processing. Catal Today 115:2–32
2. Energy, E.A.U.S.D.o. (2011) Annual Energy Review. http://www.eia.gov/totalenergy/data/annual/index.cfm. Accessed 02 May 2013
3. Tans P (2013) Trends in atmospheric carbon dioxide. www.esrl.noaa.gov/gmd/ccgg/trends/. Accessed 02 May 2013
4. Sakakura T, Kohno K (2009) The synthesis of organic carbonates from carbon dioxide. Chem Commun (Cambridge, UK) 11:1312–1330
5. Cokoja M, Bruckmeier C, Rieger B et al (2011) Transformation of carbon dioxide with homogeneous transition-metal catalysts: a molecular solution to a global challenge? Angew Chem Int Ed 50(37):8510–8537
6. Sakakura T, Choi JC, Yasuda H (2007) Transformation of carbon dioxide. Chem Rev 107:2365–2387
7. Peters M, Koehler B, Kuckshinrichs W et al (2011) Chemical technologies for exploiting and recycling carbon dioxide into the value chain. ChemSusChem 4:1216–1240
8. Darensbourg DJ, Wilson SJ (2012) What's new with CO_2? Recent advances in its copolymerization with oxiranes. Green Chem 14(10):2665–2671
9. Lu X-B, Darensbourg DJ (2012) Cobalt catalysts for the coupling of CO_2 and epoxides to provide polycarbonates and cyclic carbonates. Chem Soc Rev 41:1462–1484
10. Clements JH (2003) Reactive applications of cyclic alkylene carbonates. Ind Eng Chem Res 42:663–674
11. North M, Pasquale R, Young C (2010) Synthesis of cyclic carbonates from epoxides and CO_2. Green Chem 12(9):1514–1539
12. Varghese JK, Na SJ, Park JH et al (2010) Thermal and weathering degradation of poly (propylene carbonate). Polym Degrad Stab 95(6):1039–1044
13. Du LC, Meng YZ, Wang SJ et al (2004) Synthesis and degradation behavior of poly (propylene carbonate) derived from carbon dioxide and propylene oxide. J Appl Polym Sci 92:1840–1846
14. Luinstra GA (2008) Poly(propylene carbonate), old copolymers of propylene oxide and carbon dioxide with new interests: catalysis and material properties. Polym Rev (Philadelphia, PA, USA) 48(1):192–219
15. Qin Y, Wang X (2010) Carbon dioxide-based copolymers: environmental benefits of PPC, an industrially viable catalyst. Biotechnol J 5:1164–1180

16. Barreto C, Hansen E, Fredriksen S (2012) Novel solventless purification of poly(propylene carbonate): tailoring the composition and thermal properties of PPC. Polym Degrad Stab 97(6):893–904
17. Chisholm MH, Navarro-Llobet D, Zhou Z (2002) Poly(propylene carbonate). 1. More about poly(propylene carbonate) formed from the copolymerization of propylene oxide and carbon dioxide employing a zinc glutarate catalyst. Macromolecules 35:6494–6504
18. Kuran W, Gorecki P (1983) Degradation and depolymerization of poly(propylene carbonate) by diethylzinc. Makromol Chem 184:907–912
19. Gorecki P, Kuran W (1985) Diethylzinc-trihydric phenol catalysts for copolymerization of carbon dioxide and propylene oxide: activity in copolymerization and copolymer destruction processes. J Polym Sci Polym Lett Ed 23:299–304
20. Darensbourg DJ, Wei S-H, Wilson SJ (2013) Depolymerization of poly(indene carbonate). A unique degradation pathway. Macromolecules 46:3228–3233
21. Wang SJ, Du LC, Zhao XS et al (2002) Synthesis and characterization of alternating copolymer from carbon dioxide and propylene oxide. J Appl Polym Sci 85(11):2327–2334
22. Min SSJK, Seong JE, Na SJ et al (2008) A highly active and recyclable catalytic system for CO_2/propylene oxide copolymerization. Angew Chem Int Ed 47(38):7306–7309
23. Peng S, An Y, Chen C et al (2003) Thermal degradation kinetics of uncapped and end-capped poly(propylene carbonate). Polym Degrad Stab 80:141–147
24. Dixon DD, Ford ME, Mantell GJ (1980) Thermal stabilization of poly(alkylene carbonate)s. J Polym Sci Polym Lett Ed 18(2):131–134
25. Lai MF, Li J, Liu JJ (2005) Thermal and dynamic mechanical properties of poly(propylene carbonate). J Therm Anal Calorim 82:293–298
26. Yu T, Luo F-L, Zhao Y et al (2011) Improving the processability of biodegradable polymer by stearate additive. J Appl Polym Sci 120:692–700
27. Yao M, Mai F, Deng H et al (2011) Improved thermal stability and mechanical properties of poly(propylene carbonate) by reactive blending with maleic anhydride. J Appl Polym Sci 120:3565–3573
28. Yu T, Zhou Y, Zhao Y et al (2008) Hydrogen-bonded thermostable liquid crystalline complex formed by biodegradable polymer and amphiphilic molecules. Macromolecules 41(9):3175–3180
29. Ge XC, Zhu Q, Meng YZ (2006) Fabrication and characterization of biodegradable poly (propylene carbonate)/wood flour composites. J Appl Polym Sci 99:782–787
30. Bian J, Wei XW, Lin HL et al (2011) Preparation and characterization of modified graphite oxide/poly(propylene carbonate) composites by solution intercalation. Polym Degrad Stab 96:1833–1840
31. Shi X, Gan Z (2007) Preparation and characterization of poly(propylene carbonate)/montmorillonite nanocomposites by solution intercalation. Eur Polym J 43:4852–4858
32. Wang JT, Zhu Q, Lu XL et al (2005) ZnGA–MMT catalyzed the copolymerization of carbon dioxide with propylene oxide. Eur Polym J 41(5):1108–1114
33. Zhang Z, Lee J-H, Lee S-H et al (2008) Morphology, thermal stability and rheology of poly (propylene carbonate)/organoclay nanocomposites with different pillaring agents. Polymer 49:2947–2956
34. Chen L, Qin Y, Wang X et al (2011) Toughening of poly(propylene carbonate) by hyperbranched poly(ester-amide) via hydrogen bonding interaction. Polym Int 60:1697–1704
35. Ma X, Yu J, Wang N (2005) Compatibility characterization of poly(lactic acid)/poly(propylene carbonate) blends. J Polym Sci B 44:94–101
36. Wang N, Zhang X, Yu J et al (2008) Partially miscible poly(lactic acid)-blend-poly(propylene carbonate) filled with carbon black as conductive polymer composite. Polym Int 57:1027–1035
37. Peng S, Wang X, Dong L (2005) Special interaction between poly(propylene carbonate) and corn starch. Polym Compos 26:37–41

38. Spencer TJ, Chen Y-C, Saha R et al (2011) Stabilization of the thermal decomposition of poly (propylene carbonate) through copper ion incorporation and use in self-patterning. J Electr Mater 40:1350–1363
39. Yu T, Zhou Y, Liu K et al (2009) Improving thermal stability of biodegradable aliphatic polycarbonate by metal ion coordination. Polym Degrad Stab 94:253–258
40. Uzunlar E, Kohl PA (2012) Thermal and photocatalytic stability enhancement mechanism of poly(propylene carbonate) due to Cu(I) impurities. Polym Degrad Stab 97:1829–1837
41. Jeon JY, Lee JJ, Varghese JK et al (2012) CO_2/ethylene oxide copolymerization and ligand variation for a highly active salen-cobalt(iii) complex tethering 4 quaternary ammonium salts. Dalton Trans 42:9245–9254
42. Cyriac A, Lee SH, Varghese JK et al (2011) Preparation of flame-retarding poly(propylene carbonate). Green Chem 13(12):3469–3475
43. Cherian AE, Sun FC, Sheiko SS et al (2007) Formation of nanoparticles by intramolecular cross-linking: following the reaction progress of single polymer chains by atomic force microscopy. J Am Chem Soc 129:11350–11351
44. Cyriac A, Lee SH, Lee BY (2011) Connection of polymer chains using diepoxide in CO_2/propylene oxide copolymerizations. Polym Chem 2(4):950–956
45. Darensbourg DJ, Poland RR, Strickland AL (2012) (Salan)CrCl, an effective catalyst for the copolymerization and terpolymerization of epoxides and carbon dioxide. J Polym Sci Part A Polym Chem 50(1):127–133
46. Shi L, Lu X-B, Zhang R et al (2006) Asymmetric alternating copolymerization and terpolymerization of epoxides with carbon dioxide at mild conditions. Macromolecules 39:5679–5685
47. Darensbourg DJ, Holtcamp MW (1995) Catalytic activity of zinc(II) phenoxides which possess readily accessible coordination sites. Copolymerization and terpolymerization of epoxides and carbon dioxide. Macromolecules 28(22):7577–7579
48. Seong JE, Na SJ, Cyriac A et al (2009) Terpolymerizations of CO_2, propylene oxide, and various epoxides using a cobalt(III) complex of salen-type ligand tethered by four quaternary ammonium salts. Macromolecules 43(2):903–908
49. Harrold ND, Li Y, Chisholm MH (2013) Studies of ring-opening reactions of styrene oxide by chromium tetraphenylporphyrin initiators. Mechanistic and stereochemical considerations. Macromolecules 46(3):692–698
50. Kim JG, Cowman CD, LaPointe AM et al (2011) Tailored living block copolymerization: multiblock poly(cyclohexene carbonate)s with sequence control. Macromolecules 44(5):1110–1113
51. Darensbourg DJ, Wildeson JR, Yarbrough JC et al (2000) Bis 2,6-difluorophenoxide dimeric complexes of zinc and cadmium and their phosphine adducts: lessons learned relative to carbon dioxide/cyclohexene oxide alternating copolymerization processes catalyzed by zinc phenoxides. J Am Chem Soc 122(50):12487–12496
52. Wu G-P, Wei S-H, Lu X-B et al (2010) Highly selective synthesis of CO_2 copolymer from styrene oxide. Macromolecules 43(21):9202–9204
53. Wu G-P, Xu P-X, Lu X-B et al (2013) Crystalline CO_2 copolymer from epichlorohydrin via Co(III)-complex-mediated stereospecific polymerization. Macromolecules 46(6):2128–2133
54. Darensbourg DJ, Wilson SJ (2011) Synthesis of poly(indene carbonate) from indene oxide and carbon dioxide – a polycarbonate with a rigid backbone. J Am Chem Soc 133(46):18610–18613
55. Liu S, Xiao H, Huang K et al (2006) Terpolymerization of carbon dioxide with propylene oxide and ε-caprolactone: synthesis, characterization and biodegradability. Polym Bull 56:53–62
56. Liu Y, Huang K, Peng D et al (2006) Synthesis, characterization and hydrolysis of an aliphatic polycarbonate by terpolymerization of carbon dioxide, propylene oxide and maleic anhydride. Polymer 47(26):8453–8461

57. Hwang Y, Jung J, Ree M et al (2003) Terpolymerization of CO_2 with propylene oxide and ε-caprolactone using zinc glutarate catalyst. Macromolecules 36(22):8210–8212
58. Lu L, Huang K (2005) Synthesis and characteristics of a novel aliphatic polycarbonate, poly [(propylene oxide)-co-(carbon dioxide)-co-(γ-butyrolactone)]. Polym Int 54:870–874
59. Liu S, Wang J, Huang K et al (2011) Synthesis of poly(propylene-co-lactide carbonate) and hydrolysis of the terpolymer. Polym Bull 66:327–340
60. Wu G-P, Darensbourg DJ, Lu X-B (2012) Tandem metal-coordination copolymerization and organocatalytic ring-opening polymerization via water to synthesize diblock copolymers of styrene oxide/CO_2 and lactide. J Am Chem Soc 134:17739–17745
61. Zhang J-F, Ren W-M, Sun X-K et al (2011) Fully degradable and well-defined brush copolymers from combination of living CO_2/epoxide copolymerization, thiol-ene click reaction and ROP of ε-caprolactone. Macromolecules 44:9882–9886
62. Kröger M, Folli C, Walter O et al (2005) Alternating copolymerization of cyclohexene oxide and CO_2 catalyzed by zinc complexes with new 3-amino-2-cyanoimidoacrylate ligands. Adv Synth Catal 347(10):1325–1328
63. Lehenmeier MW, Bruckmeier C, Klaus S et al (2011) Differences in reactivity of epoxides in the copolymerisation with carbon dioxide by zinc-based catalysts: propylene oxide versus cyclohexene oxide. Chem Eur J 17(32):8858–8869
64. Kember MR, Knight PD, Reung PTR et al (2009) Highly active dizinc catalyst for the copolymerization of carbon dioxide and cyclohexene oxide at one atmosphere pressure. Angew Chem Int Ed 48:931–933
65. Seong JE, Na SJ, Cyriac A et al (2010) Terpolymerizations of CO_2, Propylene oxide, and various epoxides using a cobalt(III) complex of salen-type ligand tethered by four quaternary ammonium salts. Macromolecules 43(2):903–908
66. Ren W-M, Zhang X, Liu Y et al (2010) Highly active, bifunctional Co(III)-salen catalyst for alternating copolymerization of CO_2 with cyclohexene oxide and terpolymerization with aliphatic epoxides. Macromolecules 43:1396–1402
67. Nakano K, Kamada T, Nozaki K (2006) Selective formation of polycarbonate over cyclic carbonate: copolymerization of epoxides with carbon dioxide catalyzed by a cobalt(III) complex with a piperidinium end-capping arm. Angew Chem Int Ed 45(43):7274–7277
68. Scholl M, Ding S, Lee CW et al (1999) Synthesis and activity of a new generation of ruthenium-based olefin metathesis catalysts coordinated with 1,3-dimesityl-4,5-dihydroimidazol-2-ylidene ligands. Org Lett 1:953–956
69. Kim JG, Coates GW (2012) Synthesis and polymerization of norbornenyl-terminated multiblock poly(cyclohexene carbonate)s: a consecutive ring-opening polymerization route to multisegmented graft polycarbonates. Macromolecules 45(19):7878–7883
70. Geschwind J, Frey H (2013) Stable, hydroxyl functional polycarbonates with glycerol side chains synthesized from CO_2 and isopropylidene(glyceryl glycidyl ether). Macromol Rapid Commun 34(2):150–155
71. Cohen CT, Chu T, Coates GW (2005) Cobalt catalysts for the alternating copolymerization of propylene oxide and carbon dioxide: combining high activity and selectivity. J Am Chem Soc 127(31):10869–10878
72. Inoue S, Koinuma H, Tsuruta T (1969) Copolymerization of carbon dioxide and epoxide with organometallic compounds. Makromol Chem 130:210–220
73. Inoue S, Koinuma H, Tsuruta T (1969) Copolymerization of carbon dioxide and epoxide. J Polym Sci Part B Polym Lett 7(4):287–292
74. Aida T, Inoue S (1982) Synthesis of polyether-polycarbonate block copolymer from carbon dioxide and epoxide using a metalloporphyrin catalyst system. Macromolecules 15:682–684
75. Lednor PW, Rol NC (1985) Copolymerization of propylene oxide with carbon dioxide: a selective incorporation of propylene oxide into the polycarbonate chains, determined by 100 MHz carbon-13 NMR spectroscopy. Chem Commun (Cambridge, UK) 9:598–599
76. Nakano K, Hashimoto S, Nakamura M et al (2011) Stereocomplex of poly(propylene carbonate): synthesis of stereogradient poly(propylene carbonate) by regio- and

enantioselective copolymerization of propylene oxide with carbon dioxide. Angew Chem Int Ed 50(21):4868–4871
77. Byrnes MJ, Chisholm MH, Hadad CM et al (2004) Regioregular and regioirregular oligoether carbonates: a 13C{1H} NMR investigation. Macromolecules 37:4139–4145
78. Salmeia KA, Vagin S, Anderson CE et al (2012) Poly(propylene carbonate): insight into the microstructure and enantioselective ring-opening mechanism. Macromolecules 45:8604–8613
79. Salmeia KA (2012) Copolymerization of propylene oxide and CO_2 with salen-type catalysts; polymerization activities and polymer microstructure. Technische Universität München, Munich
80. Chisholm MH, Navarro-Llobet D, Zhou Z (2002) Poly(propylene carbonate). 1. More about poly(propylene carbonate) formed from the copolymerization of propylene oxide and carbon dioxide employing a zinc glutarate catalyst. Macromolecules 35(17):6494–6504. doi:10.1021/ma020348+
81. Ren W-M, Liu Y, Wu G-P et al (2011) Stereoregular polycarbonate synthesis: alternating copolymerization of CO_2 with aliphatic terminal epoxides catalyzed by multichiral cobalt (III) complexes. J Polym Sci Part A Polym Chem 49:4894–4901
82. Nozaki K, Nakano K, Hiyama T (1999) Optically active polycarbonates: asymmetric alternating copolymerization of cyclohexene oxide and carbon dioxide. J Am Chem Soc 121(47):11008–11009
83. Nakano K, Nozaki K, Hiyama T (2001) Spectral assignment of poly[cyclohexene oxide-alt-carbon dioxide]. Macromolecules 34(18):6325–6332
84. Nakano K, Nozaki K, Hiyama T (2003) Asymmetric alternating copolymerization of cyclohexene oxide and CO_2 with dimeric zinc complexes. J Am Chem Soc 125:5501–5510
85. Cohen CT, Thomas CM, Peretti KL et al (2006) Copolymerization of cyclohexene oxide and carbon dioxide using (salen)Co(III) complexes: synthesis and characterization of syndiotactic poly(cyclohexene carbonate). Dalton Trans 1:237–249
86. Wu G-P, Ren W-M, Luo Y et al (2012) Enhanced asymmetric induction for the copolymerization of CO_2 and cyclohexene oxide with unsymmetric enantiopure salenCo(III) complexes: synthesis of crystalline CO_2-based polycarbonate. J Am Chem Soc 134:5682–5688
87. Stevens HC (1966) High-molecular-weight polycarbonates. US 324,841
88. Klaus S, Lehenmeier MW, Anderson CE et al (2011) Recent advances in CO_2/epoxide copolymerization-new strategies and cooperative mechanisms. Coord Chem Rev 255(13–14):1460–1479
89. Takeda N, Inoue S (1978) Polymerization of 1,2-epoxypropane and copolymerization with carbon dioxide catalyzed by metalloporphyrins. Die Makromolekulare Chemie 179(5):1377–1381
90. Darensbourg DJ, Holtcamp MW, Struck GE et al (1999) Catalytic activity of a series of Zn (II) phenoxides for the copolymerization of epoxides and carbon dioxide. J Am Chem Soc 121(1):107–116
91. Moore DR, Cheng M, Lobkovsky EB et al (2002) Electronic and steric effects on catalysts for CO_2/epoxide polymerization: subtle modifications resulting in superior activities. Angew Chem Int Ed 41(14):2599–2602
92. Darensbourg DJ (2010) Chemistry of carbon dioxide relevant to its utilization: a personal perspective. Inorg Chem (Washington, DC, USA) 49(23):10765–10780
93. Darensbourg DJ (2007) Making plastics from carbon dioxide: salen metal complexes as catalysts for the production of polycarbonates from epoxides and CO_2. Chem Rev 107(6):2388–2410
94. Kember MR, Buchard A, Williams CK (2011) Catalysts for CO_2/epoxide copolymerization. Chem Commun (Cambridge, UK) 47(1):141–163
95. Ikpo N, Flogeras JC, Kerton FM (2013) Aluminium coordination complexes in copolymerization reactions of carbon dioxide and epoxides. Dalton Trans 42:8998–9006

96. Sugimoto H, Inoue S (2004) Copolymerization of carbon dioxide and epoxide. J Polymr Sci Part A Polym Chem 42(22):5561–5573
97. Coates GW, Moore DR (2004) Discrete metal-based catalysts for the copolymerization of CO_2 and epoxides: discovery, reactivity, optimization, and mechanism. Angew Chem Int Ed 43(48):6618–6639
98. Hansen KB, Leighton JL, Jacobsen EN (1996) On the mechanism of asymmetric nucleophilic ring-opening of epoxides catalyzed by (Salen)CrIII complexes. J Am Chem Soc 118:10924–10925
99. Luinstra GA, Haas GR, Molnar F et al (2005) On the formation of aliphatic polycarbonates from epoxides with chromium(III) and aluminum(III) metal-salen complexes. Chem Eur J 11:6298–6314
100. Darensbourg DJ, Yarbrough JC (2002) Mechanistic aspects of the copolymerization reaction of carbon dioxide and epoxides, using a chiral salen chromium chloride catalyst. J Am Chem Soc 124(22):6335–6342
101. Darensbourg DJ, Yarbrough JC, Ortiz C et al (2003) Comparative kinetic studies of the copolymerization of cyclohexene oxide and propylene oxide with carbon dioxide in the presence of chromium salen derivatives. In situ FTIR measurements of copolymer vs cyclic carbonate production. J Am Chem Soc 125(25):7586–7591
102. Darensbourg DJ, Rodgers JL, Mackiewicz RM et al (2004) Probing the mechanistic aspects of the chromium salen catalyzed carbon dioxide/epoxide copolymerization process using in situ ATR/FTIR. Catal Today 98(4):485–492
103. Rao D-Y, Li B, Zhang R et al (2009) Binding of 4-(N, N-dimethylamino)pyridine to Salen- and Salan-Cr(III) cations: a mechanistic understanding on the difference in their catalytic activity for CO2/epoxide copolymerization. Inorg Chem (Washington, DC, USA) 48:2830–2836
104. Lu X-B, Wang Y (2004) Highly active, binary catalyst systems for the alternating copolymerization of CO_2 and epoxides under mild conditions. Angew Chem Int Ed 43:3574–3577
105. Lu X-B, Shi L, Wang Y-M et al (2006) Design of highly active binary catalyst systems for CO_2/epoxide copolymerization: polymer selectivity, enantioselectivity, and stereochemistry control. J Am Chem Soc 128(5):1664–1674
106. Cohen CT, Coates GW (2006) Alternating copolymerization of propylene oxide and carbon dioxide with highly efficient and selective (salen)Co(III) catalysts: effect of ligand and cocatalyst variation. J Polym Sci Part A Polym Chem 44(17):5182–5191
107. Niu Y, Zhang W, Pang X et al (2007) Alternating copolymerization of carbon dioxide and propylene oxide catalyzed by (R, R)-SalenCoIII-(2,4-dinitrophenoxy) and Lewis-basic cocatalyst. J Polym Sci Part A Polym Chem 45(22):5050–5056
108. Qin Z, Thomas CM, Lee S et al (2003) Cobalt-based complexes for the copolymerization of propylene oxide and CO_2: active and for polycarbonate synthesis. Angew Chem Int Ed 42(44):5484–5487
109. Sugimoto H, Kuroda K (2008) The cobalt porphyrin-lewis base system: a highly selective catalyst for alternating copolymerization of CO_2 and epoxide under mild conditions. Macromolecules 41:312–317
110. Guo L, Wang C, Zhao W et al (2009) Copolymerization of CO_2 and cyclohexene oxide using a lysine-based (salen)CrIIICl catalyst. Dalton Trans 27:5406–5410
111. Darensbourg DJ, Bottarelli P, Andreatta JR (2007) Inquiry into the formation of cyclic carbonates during the (salen)CrX catalyzed CO_2/cyclohexene oxide copolymerization process in the presence of ionic initiators. Macromolecules 40(21):7727–7729
112. Darensbourg DJ, Phelps AL (2005) Effective, selective coupling of propylene oxide and carbon dioxide to poly(propylene carbonate) using (salen)CrN3 catalysts. Inorg Chem (Washington, DC, USA) 44(13):4622–4629
113. Darensbourg DJ, Mackiewicz RM (2005) Role of the cocatalyst in the copolymerization of CO_2 and cyclohexene oxide utilizing chromium salen complexes. J Am Chem Soc 127(40):14026–14038

114. Eberhardt R, Allmendinger M, Rieger B (2003) DMAP [4-(N, N-dimethylamino)pyridine]/Cr(III) catalyst ratio: the decisive factor for poly(propylene carbonate) formation in the coupling of CO_2 and propylene oxide. Macromol Rapid Commun 24(2):194–196
115. Darensbourg DJ, Mackiewicz RM, Rodgers JL et al (2004) Cyclohexene oxide/CO_2 copolymerization catalyzed by chromium(III) salen complexes and N-methylimidazole: effects of varying salen ligand substituents and relative cocatalyst loading. Inorg Chem (Washington, DC, USA) 43:6024–6034
116. Darensbourg DJ, Mackiewicz RM, Rodgers JL et al (2004) (Salen)CrIIIX catalysts for the copolymerization of carbon dioxide and epoxides: role of the initiator and cocatalyst. Inorg Chem (Washington, DC, USA) 43:1831–1833
117. Moore DR, Cheng M, Lobkovsky EB et al (2003) Mechanism of the alternating copolymerization of epoxides and CO_2 using β-diiminate zinc catalysts: evidence for a bimetallic epoxide enchainment. J Am Chem Soc 125(39):11911–11924
118. Cyriac A, Lee SH, Varghese JK et al (2010) Immortal CO_2/propylene oxide copolymerization: precise control of molecular weight and architecture of various block copolymers. Macromolecules 43(18):7398–7401
119. Noh EK, Na SJ, Sujith S et al (2007) Two components in a molecule: highly efficient and thermally robust catalytic system for CO_2/epoxide copolymerization. J Am Chem Soc 129 (26):8082–8083
120. Yoo J, Na SJ, Park HC et al (2010) Anion variation on a cobalt(III) complex of salen-type ligand tethered by four quaternary ammonium salts for CO_2/epoxide copolymerization. Dalton Trans 39(10):2622–2630
121. Na Sung J, Sujith S, Cyriac A et al (2009) Elucidation of the structure of a highly active catalytic system for CO_2/epoxide copolymerization: a salen-cobaltate complex of an unusual binding mode. Inorg Chem (Washington, DC, USA) 48(21):10455–10465
122. Ren W-M, Liu Z-W, Wen Y-Q et al (2009) Mechanistic aspects of the copolymerization of CO_2 with epoxides using a thermally stable single-site cobalt(III) catalyst. J Am Chem Soc 131(32):11509–11518
123. Zheng YQ, Lin JL, Zhang HL (2000) Crystal structure of zinc glutarate, Zn(C5H6O4). Zeitschrift fuer Kristallographie – New Crystal Struct 215(4):535–536
124. Ree M, Hwang Y, Kim J-S et al (2006) New findings in the catalytic activity of zinc glutarate and its application in the chemical fixation of CO_2 into polycarbonates and their derivatives. Catal Today 115:134–145
125. Eberhardt R, Allmendinger M, Zintl M et al (2004) New zinc dicarboxylate catalysts for the CO_2/propylene oxide copolymerization reaction: activity enhancement through zn(II)-ethylsulfinate initiating groups. Macromol Chem Phys 205(1):42–47
126. Zhu Q, Meng YZ, Tjong SC et al (2003) Catalytic synthesis and characterization of an alternating copolymer from carbon dioxide and propylene oxide using zinc pimelite. Polymer Int 52:799–804
127. Wang JT, Shu D, Xiao M et al (2006) Copolymerization of carbon dioxide and propylene oxide using zinc adipate as catalyst. J Appl Polym Sci 99:200–206
128. Klaus S, Lehenmeier MW, Herdtweck E et al (2011) Mechanistic insights into heterogeneous zinc dicarboxylates and theoretical considerations for CO_2-epoxide copolymerization. J Am Chem Soc 133:13151–13161
129. Lehenmeier M (2012) Synthese zweikerniger Zinkkatalysatoren zur Copolymerisation von Kohlenstoffdioxid und Epoxiden. Technische Universität München, Munich
130. Van Meerendonk WJ, Duchateau R, Koning CE et al (2005) Unexpected side reactions and chain transfer for zinc-catalyzed copolymerization of cyclohexene oxide and carbon dioxide. Macromolecules 38(17):7306–7313
131. Allen SD, Moore DR, Lobkovsky EB et al (2002) High-activity, single-site catalysts for the alternating copolymerization of CO_2 and propylene oxide. J Am Chem Soc 124(48):14284–14285

132. Rieth LR, Moore DR, Lobkovsky EB et al (2002) Single-site β-diiminate zinc catalysts for the ring-opening polymerization of β-butyrolactone and β-valerolactone to poly (3-hydroxyalkanoates). J Am Chem Soc 124:15239–15248
133. Eberhardt R, Allmendinger M, Luinstra GA et al (2003) The ethylsulfinate ligand: a highly efficient initiating group for the zinc β-diiminate catalyzed copolymerization reaction of CO_2 and epoxides. Organometallics 22:211–214
134. Lee BY, Kwon HY, Lee SY et al (2005) Bimetallic anilido-aldimine zinc complexes for epoxide/CO_2 copolymerization. J Am Chem Soc 127(9):3031–3037
135. Bok T, Yun H, Lee BY (2006) Bimetallic fluorine-substituted anilido-aldimine zinc complexes for CO_2/(cyclohexene oxide) copolymerization. Inorg Chem (Washington, DC, USA) 45(10):4228–4237
136. Jutz F, Buchard A, Kember MR et al (2011) Mechanistic investigation and reaction kinetics of the low-pressure copolymerization of cyclohexene oxide and carbon dioxide catalyzed by a dizinc complex. J Am Chem Soc 133(43):17395–17405
137. Kember MR, White AJP, Williams CK (2010) Highly active di- and trimetallic cobalt catalysts for the copolymerization of CHO and CO_2 at atmospheric pressure. Macromolecules 43:2291–2298
138. Buchard A, Kember MR, Sandeman KG et al (2011) A bimetallic iron(III) catalyst for CO_2/epoxide coupling. Chem Commun (Cambridge, UK) 47:212–214
139. Kember MR, Williams CK (2012) Efficient magnesium catalysts for the copolymerization of epoxides and CO_2; using water to synthesize polycarbonate polyols. J Am Chem Soc 134 (38):15676–15679
140. Lehenmeier MW, Kissling S, Altenbuchner PT et al (2013) Flexibly tethered dinuclear zinc complexes: a solution to the entropy problem in CO_2/epoxide copolymerization catalysis? Angew Chem Int Ed 52(37):9821–9826